



Submitted:
01.08.2023
Accepted:
28.09.2023
Published:
30.10.2023

High-resolution ultrasound and MRI in the evaluation of the forefoot and midfoot

Monique Reijnierse¹, James F. Griffith²

¹ Department of Radiology, Leiden University Medical Center, Leiden, Netherlands

² Department of Imaging & Interventional Radiology, The Chinese University of Hong Kong, Prince of Wales Hospital, Hong Kong

Corresponding author: Monique Reijnierse; e-mail: m.reijnierse@lumc.nl

DOI: 10.15557/JoU.2023.0033

Keywords

rheumatoid arthritis;
ultrasound;
MRI;
forefoot;
plantar plate

Abstract

Radiography is the appropriate initial imaging modality to assess for midfoot and forefoot pathology before turning to advanced imaging techniques. While most lesions of the mid- and forefoot can be diagnosed clinically, the exact nature and severity of the pathology is often unclear. This review addresses the use of the ultrasound, as well as the added value of magnetic resonance imaging, in diagnosing conditions of the mid-foot and forefoot. Ultrasound allows a dynamic assessment as well as enabling imaging-guided interventions for diagnostic and therapeutic purposes. Practical tips for optimal examination of this area with ultrasound and magnetic resonance imaging are provided. Metatarsal stress fracture, Chopart's injury, Lisfranc injury, as well as the 1st metatarsophalangeal joint injury and lesser metatarsophalangeal plantar plate injury are injuries unique to the mid- and forefoot. The imaging anatomy of the 1st and lesser metatarsophalangeal joints is reviewed, as such knowledge is key to correctly assessing injury of these joints. Characteristic imaging features of masses commonly encountered in the mid- and forefoot, such as ganglion cyst, Morton neuroma, gouty tophus, plantar fibroma, foreign body granuloma, and leiomyoma are reviewed. The use of ultrasound and magnetic resonance imaging in assessing degenerative and inflammatory joint disorders, and in particular rheumatoid arthritis, of the mid- and forefoot region is also reviewed. In summary, when necessary, most lesions of the mid- and forefoot can be adequately assessed with ultrasound, supplemented on occasion with radiographs, computed tomography, or magnetic resonance imaging.

Introduction

The relatively superficial location and high innervation of the mid- and forefoot allows good clinical location of most pathologies, but the exact nature and severity of the pathology is often unclear. The superficial location of most mid- and forefoot structures also facilitates assessment by ultrasound (US). The only areas limited to assessment by US are the internal joint areas, the subcortical parts of bones, and the deeper soft tissues on the plantar aspect of the midfoot.

Radiographs, as a first-line investigation, are usually sufficient to fully evaluate most traumatic fractures or dislocations of the mid- and forefoot. Weight-bearing radiographs, while helpful, are not always achievable in some painful, post-traumatic conditions. Coned oblique radiographs may be useful in evaluating sesamoid

pathology. For most other conditions, US is the next best imaging investigation. In general, the more precise the symptom location, the greater the benefit of US examination. In most cases, US allows determination of both (a) the exact anatomical site of pathology and (b) the precise nature and severity of this pathology.

Advanced US techniques (e.g. elastography, contrast enhancement) are usually not necessary. US also facilitates diagnostic maneuvers such as fluid aspiration for culture and sensitivity and crystal analysis, percutaneous biopsy, or therapeutic maneuvers such as corticosteroid injection of a joint, tendon sheath, or around Morton's neuromas. When US fails to adequately identify or fully assess the underlying pathology, magnetic resonance imaging (MRI) with or without computed tomography (CT) are helpful ancillary investigations. Table 1 and Tab. 2 outline practical tips to optimize US and MRI examinations of the mid- and forefoot.

Tab. 1. Ultrasound technique tips for examination of the mid- and forefoot

- Ensure both you and the patient are in a comfortable position to adequately examine the mid- and hindfoot. Examination of the dorsum or plantar aspect of the foot is normally performed with the foot resting on the examination table, as shown in Fig. 1.
- Review any radiographs. Take a history and palpate any lump, if present.
- Use a linear high resolution (7–18 MHz) linear transducer. Higher resolution transducers such as a ‘hockey stick’ (18 MHz) or 25 MHz transducer can be used to improve the resolution of smaller structures.
- Use of copious acoustic gel to minimize air gap interference.
- Start by examining the corresponding area on the contralateral unaffected foot. This enables one to assess normal anatomy for that part and set up the transducer optimally.
- Ensure optimization of transducer depth, focal zone, and time-gain curve settings.
- Use compressibility and dynamic assessment for tendon, ligament, or plantar plate assessment
- Applied specific maneuvers such as Mulder’s maneuver, when appropriate.
- Use minimal transducer pressure when assessing vascularity of superficial structures with color Doppler imaging.
- Ensure that the abnormality found on US examination concurs with the clinical symptoms. If the pathology does not fully explain the clinical symptoms or if the lesion has not been fully evaluated, arrange an alternative imaging examination, which will usually be MRI.
- Use a full aseptic technique, including a sterile transducer cover, for any interventional procedures.

Tab. 2. MRI technique tips for examination of the mid- and forefoot

- Use a dedicated coil, such as an ‘ankle and foot’ coil or a flexible surface coil. The larger dedicated foot and ankle coil enables the examination to be extended to the ankle region, if necessary, and also helps minimize movement artifacts.
- Small field-of-view coils are helpful for localized pathology e.g. subungual glomus tumor.
- Due to the small structures involved and the need for high-resolution imaging, 3T imaging is preferable to 1.5T imaging, if available.
- A combination of coronal and sagittal with or without oblique axial sequences are used.
- T1W and T2W FS sequences are most commonly used.
- Dixon technique is useful to acquire homogeneous imaging as well as the simultaneous acquisition of water and fat images.
- Oblique axial imaging parallel to the metatarsal shafts is especially helpful if mid-foot bone pathology, such as osteomyelitis or stress fracture, is suspected.
- Intravenous contrast may be helpful to assess the presence of collections within an inflammatory mass, to assess synovitis and vascular tumor. Most MRI examinations can be adequately performed without intravenous contrast.
- T1W FS or subtraction images may be helpful before and after contrast administration.
- Dynamic contrast-enhanced MRI imaging or other functional imaging techniques are generally not necessary for MRI assessment of the mid- and forefoot.

Osseous injury

Stress fracture and other bony non-tumoral pathology

Stress fractures typically occur in young to middle-aged individuals undertaking unaccustomed high levels of exercise over an extended period. The 2nd and, less frequently, the 3rd metatarsal mid-shafts are commonly affected sites⁽¹⁾ (Fig. 1). The base of the 2nd metatarsal is splinted between the distal end of the medial cuneiform and the 3rd metatarsal bone. It is also a key weight-bearing bone, making it more susceptible to injury. The 1st, 2nd and 5th metatarsal bases, the navicular, cuneiform, cuboid, and medial sesamoid bones are additional common sites of stress fractures in the mid- and forefoot^(1,2) (Fig. 2). Radiographs are normal in the earliest stages of stress fracture. US at this juncture may reveal a cuff of echogenic thickening due to thickened periosteum (‘periostitis’) around the cortex of the affected bone area. The cortex may be less distinct than usual, together with juxtacortical soft tissue edema and hyperemia (Fig. 1). While such findings are non-specific, they are usually diagnostic in the appropriate clinical setting without the need for additional imaging other than radiographic follow-up. MRI will provide even earlier detection of stress fracture than US, revealing focal bone marrow edema (BME) at the affected site, often with a thin hypointense

fracture line⁽¹⁾ (Fig. 2). In the appropriate clinical setting, BME on fat-suppressed, fluid-sensitive sequences without a visible fracture line is termed a ‘stress reaction’ rather than a ‘stress fracture’⁽¹⁾. Radiographs and US will typically be normal in stress reaction. It is important to correlate any BME with clinical symptoms, as BME may occur due to physiological bone remodeling without necessarily being reflective of an injurious stress reaction⁽³⁾.

Sesamoid pathology

Sesamoid pathology is quite common and includes osteoarthritis of the sesamoid-first metatarsophalangeal (MTP) articulation, traumatic sesamoid bone fracture, and sesamoid bone stress fracture and sesamoid bone inflammation, known as sesamoiditis, which may be secondary to either stress reaction or osteonecrosis⁽⁴⁾. Osteoarthritis between the sesamoid and the undersurface of the first metatarsal head articulation is usually assessed radiographically. Sesamoid fracture is also evaluated by radiography and should be distinguished from a bipartite sesamoid bone (Fig. 3). In bipartite sesamoid, the summated size of both sesamoid components is greater than the expected size of the sesamoid bone. Also, the opposing bone edges are smooth and corticated, with a transversely orientated partition, as opposed to the often irregular, obliquely orientated

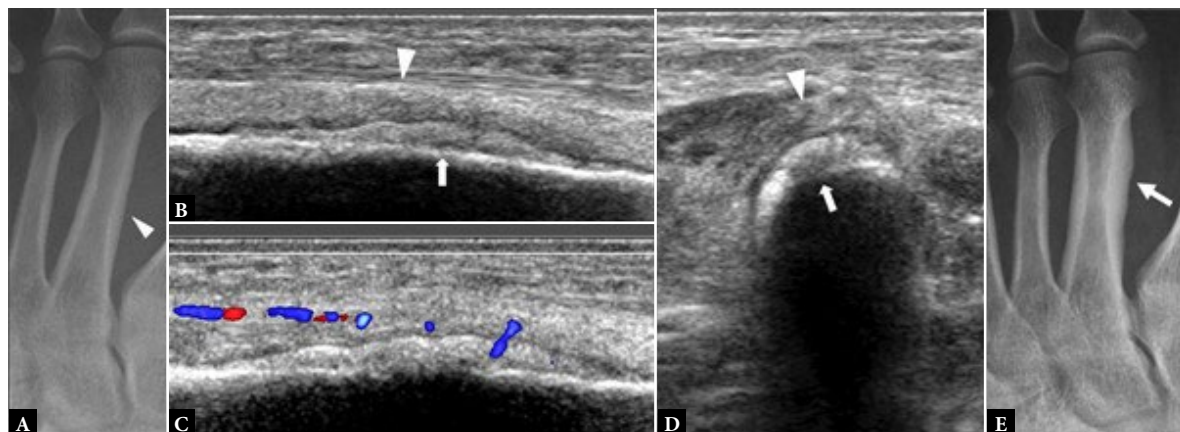


Fig. 1. 41-year-old female with forefoot pain and swelling for one month. There was no specific traumatic event and no undue sporting activity. A tendon injury was suspected clinically **A.** Dorsoplantar (DP) radiograph shows normal 2nd metatarsal bone (arrowhead). **B.** Longitudinal greyscale and **C.** color Doppler, and **D.** transverse greyscale US images show moderate severity localized periosteal thickening (open arrow) of the 2nd metatarsal shaft dorsally, with moderate adjacent soft tissue thickening (open arrowhead) consistent with active stress fracture. **E.** Radiograph three months later showed marked periosteal thickening of the 2nd metatarsal shaft (arrow) compatible with healed stress fracture

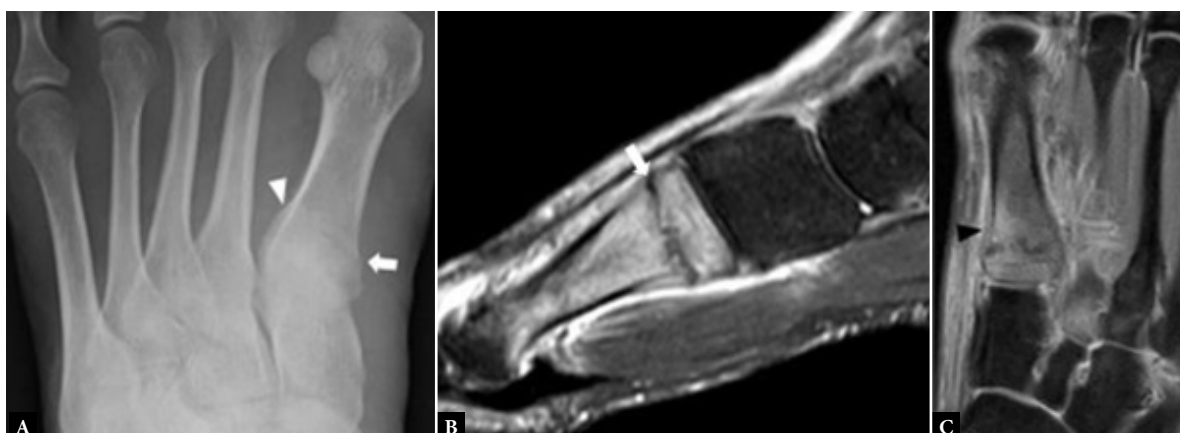
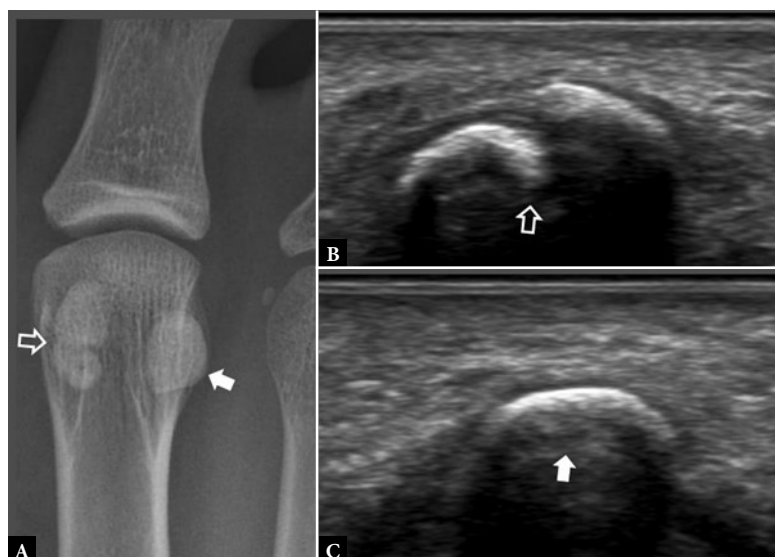


Fig. 2. 41-year-old female recreational runner with medial forefoot pain for one month. There was no specific traumatic event. **A.** Dorsoplantar radiograph shows solid periosteal thickening (arrowhead) base of 1st metatarsal bone as well as faint transverse fracture line (arrow). **B.** Sagittal and **C.** axial T2WFS image forefoot showing nondisplaced transverse fracture (arrow) base of 1st metatarsal bone with severe bone marrow edema, mild periosteal thickening (arrowhead) and moderate surrounding soft tissue edema. The acuteness of the fracture can be appreciated much better on MR than radiographs

Fig. 3. 32-year-old female with medial forefoot pain. **A.** Dorsoplantar radiograph of the first MTP joint shows a bipartite medial sesamoid bone (open arrow), which is longer than the lateral sesamoid bone (arrow). **B.** Longitudinal greyscale US image of bipartite medial sesamoid bone (open arrow). There is no surrounding soft tissue edema to indicate recent fracture. **C.** Longitudinal US image of lateral sesamoid bone (arrow) on the same side. This bipartite sesamoid bone was an incidental finding, unrelated to the patient's symptoms



margins of a sesamoid fracture (Fig. 4). Sesamoiditis is seen on MRI examination as diffuse edema of the affected sesamoid bone.

Freiberg's disease is an infraction that most likely follows a subchondral fracture, leading to progressive flattening and collapse most commonly of the second metatarsal head, though the other lesser metatarsal heads may also be affected (Fig. 5). It is about five

times more common in females. The diagnosis is usually made radiographically and supported, if necessary, by CT or MRI as a prelude to osteotomy⁽⁵⁾. US may potentially help in detecting Freiberg's disease when radiographs are not available with assessment of inflammation, synovial hypertrophy and hyperemia on Doppler imaging, at the 2nd metatarsophalangeal joint. Otherwise, the role of US in Freiberg's disease is limited.



Fig. 4. 16-year-old female with recent pain plantar aspect 1st MTP joint following a gymnastics tournament. **A.** Dorsoplantar radiograph of 1st MTP joint shows irregular transverse fracture medial sesamoid bone (open arrow). **B.** For comparison, on a dorsoplantar radiograph of the contralateral, asymptomatic 1st MTP joint, the medial sesamoid bone is normal (arrow)



Fig. 5. 29-year-old man with forefoot pain for nine months. Dorsoplantar radiograph of the forefoot shows established Freiberg's disease of second metatarsal head (open arrow). T1W **B.** sagittal and **C.** axial MR images of same patient show moderate collapse of the metatarsal head (arrows), with moderate secondary osteoarthritis of the second MTP joint. **D.** T2W FS axial MR image of the same region shows moderate sub-articular bone marrow edema surrounding the second MTP joint (arrow)

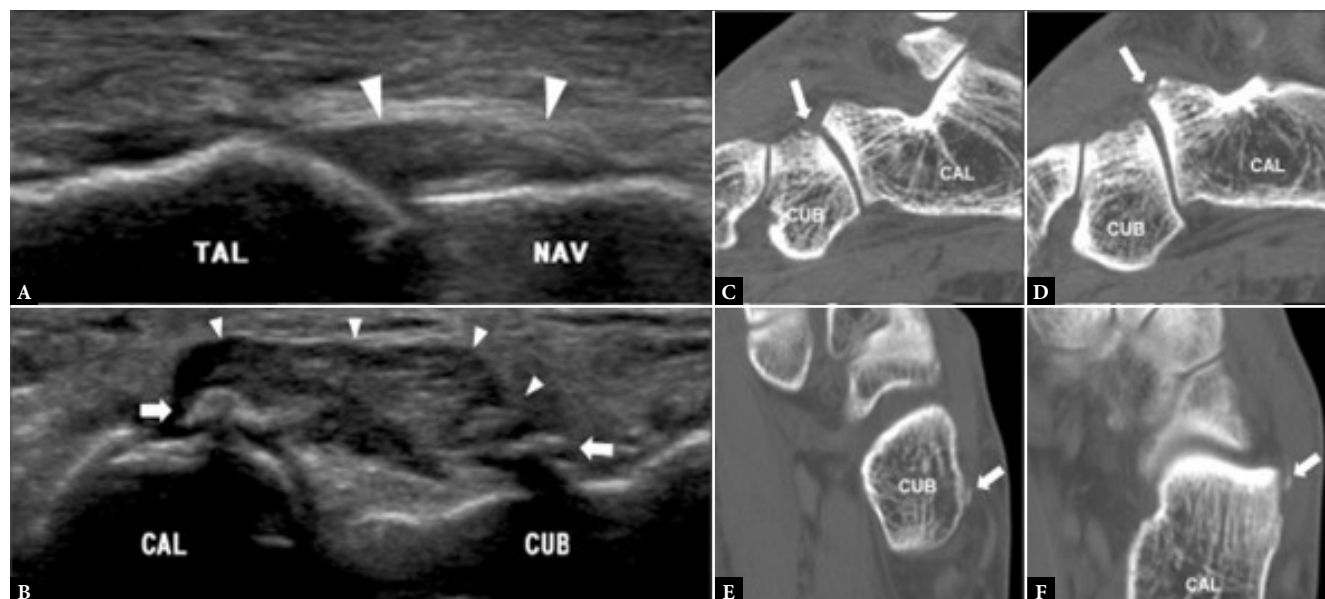


Fig. 6. 48-year-old woman with midfoot sprain. Longitudinal greyscale US images of Index Chopart's joint show **A.** moderate severity swelling indicative of sprain of the dorsal talonavicular ligament (arrowheads) between the talar head (TAL) and the navicular bone (NAV) and **B.** severe tear of the dorsal calcaneocuboid ligament (arrowheads) with avulsion fractures (arrows) from the calcaneum (CAL) and cuboid (CUB) bones. US also showed additional avulsion fractures and a moderate-severity anterior talofibular ligament tear (not shown). Corresponding CT with **C, D.** sagittal and **E, F.** axial reconstructions shows several small calcaneal (CAL) and cuboid (CUB) avulsion fractures (arrows)

Ligament injury

Although clinical symptoms are often severe, ligamentous injury of Chopart's and Lisfranc joints is often associated with only minor bony avulsions or subtle bony malalignment. Hence, both injuries tend to be overlooked if not specifically considered.

Chopart's injury usually occurs from a midfoot inversion injury ('mid-foot sprain'), often in conjunction with a lateral ankle ligament tear. Tears, often accompanied by small bony avulsions, occur at the dorsal calcaneocuboid, bifurcate, and dorsal talonavicular ligaments (Fig. 6)⁽⁶⁾. US is an effective screening examination for such injuries⁽⁶⁾, and a combination of radiographs and US usually provides sufficient assessment for clinical management. CT and MRI enable a fuller assessment if clinically warranted as in, for example, high-performance athletes (Fig. 6). CT readily depicts the full range of avulsion fractures, while MRI may reveal concomitant variable BME as a feature of disease activity.

Lisfranc trauma ranges from ligamentous injury to complex fracture-dislocations. It may occur acutely, following high-speed injury, or insidiously, as in diabetic midfoot osteoarthropathy. The Lisfranc ligament complex has three components, with the interosseous component being the strongest and the dorsal component being the weakest (Fig. 7, Fig. 8)⁽⁷⁾. The strong intercuneiform ligament between the medial and intermediate cuneiform bones also indirectly helps stabilize the Lisfranc articulation⁽⁷⁾. In patients undergoing surgery for suspected Lisfranc injury, the interosseous Lisfranc ligament was torn in 100%, the dorsal component was torn in 75%, and the intercuneiform ligament was torn in 25%⁽⁷⁾. Ligament injury can be isolated or associated with severe fracture-dislocation. Conventional foot radiographs are the first-line imaging modality. In patients with high energy trauma, the diagnosis is usually obvious, and CT will help with surgical planning⁽⁸⁾. In patients with low-energy injury, bilateral weight-bearing radiographs are helpful at detecting

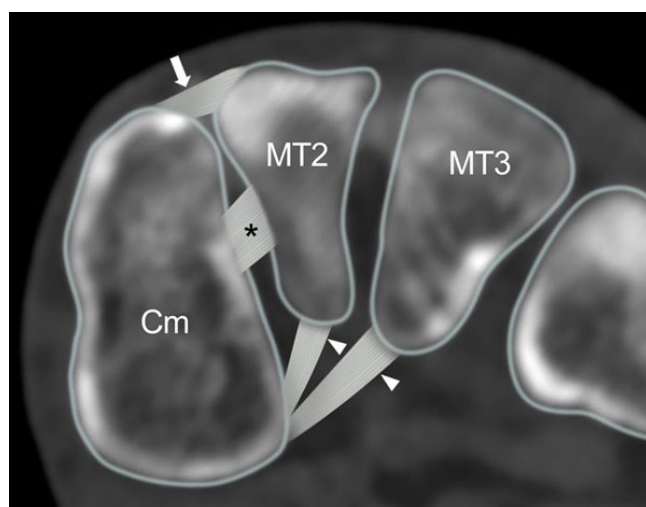


Fig. 7. Schematic diagram of Lisfranc ligament complex shows dorsal (arrow), interosseous (*) and plantar (arrowheads) components of Lisfranc ligament. Cm, medial cuneiform, MT2, second metatarsal base, MT3, 3rd metatarsal base

subtle subluxation, though obtaining standing radiographs is often impractical in the acute setting. CT will reveal nondisplaced fractures and subtle subluxation that may be overlooked radiographically (Fig. 9)⁽⁸⁾. Weight-bearing CT is also feasible⁽⁹⁾. On ultrasound, only the dorsal component of the Lisfranc ligament can be reliably seen. Both feet should be compared. Ultrasound signs of a Lisfranc injury include a thickened or absent dorsal ligament, with or without a medial cuneiform-2nd metatarsal distance of >2.5 mm which may further widen on weight-bearing⁽¹⁰⁾. A normal dorsal Lisfranc ligament does not exclude additional ligament injury⁽⁸⁾. MRI reliably demonstrates all of the Lisfranc and inter-cuneiform ligaments and is the non-operative gold standard for diagnosing ligament injury (Fig. 8)⁽⁸⁾.

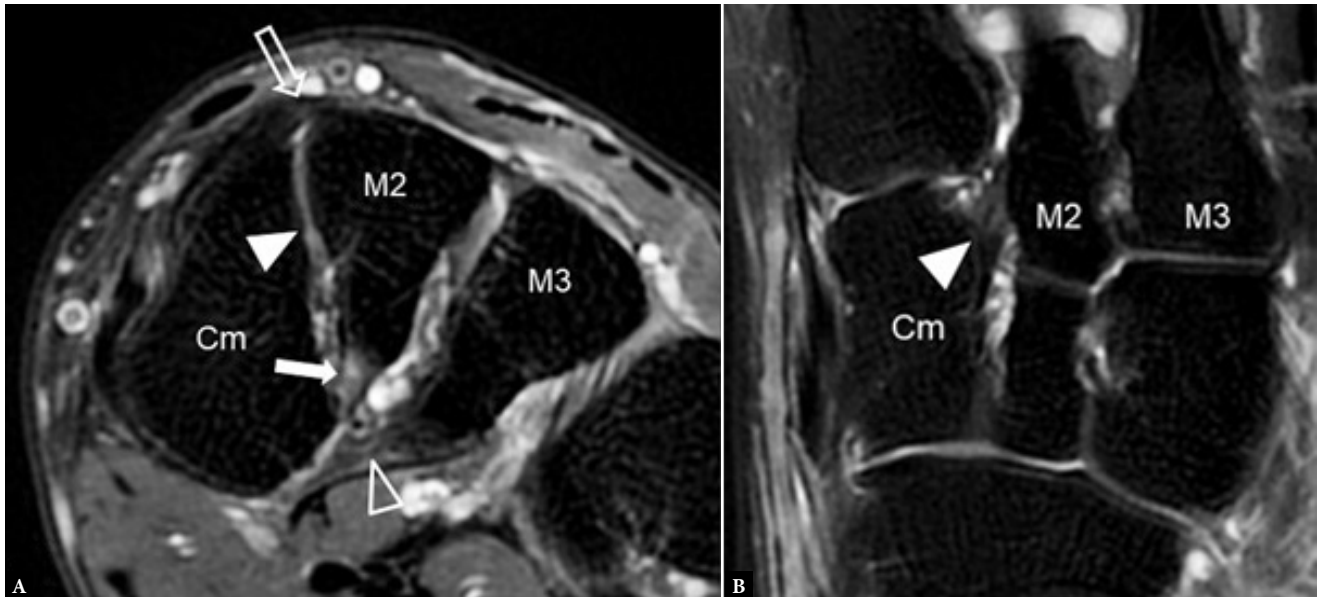


Fig. 8. 49-year-old man with medial forefoot pain following injury. Lisfranc injury was suspected clinically. T2-fat suppressed **A.** coronal MR image shows a moderately edematous cuneiform-2nd metatarsal ligament (arrow) without a discrete tear consistent with a moderate-severity sprain. The dorsal ligament (open arrow), interosseous Lisfranc ligament (closed arrowhead), and cuneiform-3rd metatarsal ligament (open arrowhead) are all intact. **B.** T2-fat suppressed axial MR image in the same patient shows the intact interosseous Lisfranc ligament (closed arrowhead)



Fig. 9. 33-year-old man with midfoot pain and swelling following road vehicle accident. **A.** Dorsoplantar radiograph of normal foot. The second metatarsal base is normally aligned perfectly with the intermediate cuneiform bone. **B.** Dorsoplantar radiograph of injured foot shows mild lateral offset of the second metatarsal base relative to the intermediate cuneiform bone (arrow) indicative of a Lisfranc subluxation. There is also a fracture of the first metatarsal base. **C.** Corresponding axial CT reconstruction confirms offset at the base of second metatarsal base (arrow) with an angulated subluxation and fracture of the first metatarsal base (convergent Lisfranc subluxation). Diastasis between the medial cuneiform bone (C1) and the 2nd metatarsal base (MT2) is also more apparent on CT than radiograph

Other soft tissue injuries

First metatarsophalangeal (MTP) joint injury (“Turf Toe”)

Injury to the 1st MTP joint, which is broadly termed ‘turf toe’, is common among athletes⁽⁴⁾. As the anatomy of the first MTP joint differs from that of the lesser MTP joints, the injury spectrum also differs. The first MTP joint contains the paired sesamoid bones which are held in place by a framework of ligament, tendon, capsule, and fi-

brocartilaginous plantar plate attachments (Fig. 10, Fig. 11). The plantar plate is a trapezoidal-shaped thickening on the plantar aspect of the MTP joint (Fig. 10, Fig. 11). Distally, it is attached to the proximal phalanx and proximally to the inter-sesamoid ligament (Fig. 10, Fig. 11). As the 1st MTP joint anatomy is rather complex, plantar plate and ligament injury is usually best assessed with MRI rather than with US.

The plantar plate is the most frequently injured component of the 1st MTP joint though other supporting structures can also be torn

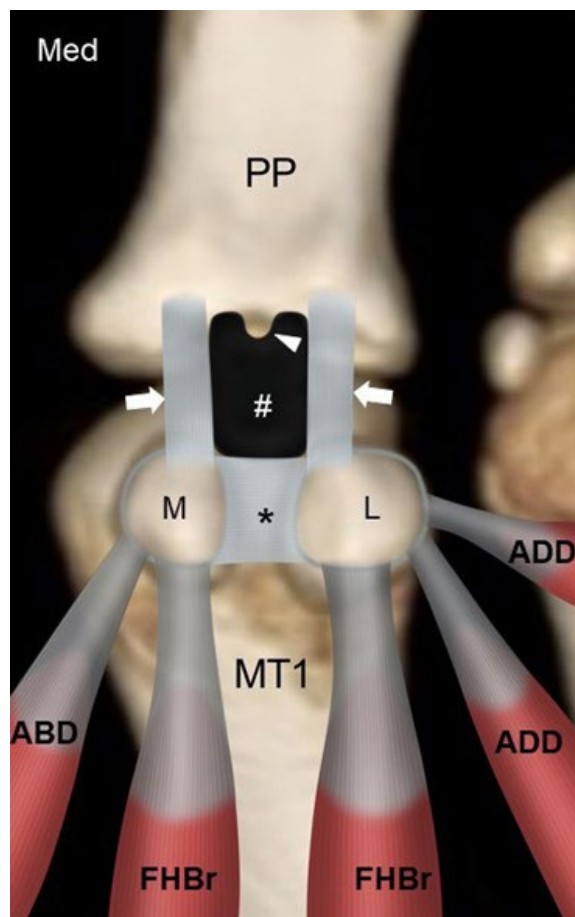


Fig. 10. Schematic diagram plantar aspect 1st MTP joint shows the medial (M) and lateral (L) sesamoid bones held in place by the abductor hallucis (ABD), medial and lateral heads of flexor hallucis brevis (FHB), oblique and transverse heads of adductor hallucis (ADD) tendons as well as the inter-sesamoid ligament (*) and medial and lateral sesamoid-phalangeal ligaments (arrows). The sesamoids are also supported by the paired medial and lateral metatarsal- sesamoid ligaments (not shown). The plantar plate (#) with a small distal central recess (arrowhead) is also shown. (Med, medial; PP, proximal phalanx, MT1, 1st metatarsal bone)

either in isolation or in conjunction with a plantar plate tear. Plantar plate injury may be acute from traumatic hyperextension or chronic. The relative prevalence of acute or chronic tears seen is largely dependent on the referral population. Chronic tears occur in degenerative attenuated plantar plates from repetitive overload (Fig. 12). On MRI, degenerated plantar plates will tend to have intermediate rather than low signal intensity on all pulse sequences⁽¹¹⁾. Partial tears are more common than complete tears. If complete tears are accompanied by tearing of the supporting sesamoid ligaments, proximal migration of one or both sesamoid bones may occur. Unlike plantar plate tears of the lesser MTP joints, 1st MTP joint plantar plate tears tend not to induce exuberant reactive capsular/pericapsular fibrosis.

Lesser MTP joint plantar plate tear

Even more so than the 1st MTP joint, the plantar plates of the lesser MTP joints resist joint hyperextension and provide sagittal stability⁽¹¹⁾. Distally, the plantar plates are firmly attached to the proximal phalangeal bases while proximally, they are loosely attached to the metacarpal necks by fibro-synovial tissue⁽¹²⁾. On either side, the plantar plates are firmly attached to the medial and lateral accessory collateral ligaments (Fig. 13) and, as such, co-existent injury of the plantar plate and accessory ligaments commonly occurs⁽¹²⁾. Plantar plate tear can lead to MTP joint medial or lateral deviation, dorsal subluxation, and hammer toe⁽¹³⁾. The normal plantar plate and plate tears are shown on US and MRI in Fig. 14 and Fig. 15. As with the 1st MTP joint, a midline hyperintense zone, measuring up to 2.5 mm long, at the phalangeal base is a normal anatomic recess⁽¹¹⁾ (Fig. 10). This is less frequently appreciated on US as a hyperechoic zone.

The 2nd, followed by the 3rd, MTP joint plantar plates are the most frequently injured⁽¹²⁾. Plantar plate tears typically occur at the junction between the plantar plate and the accessory collateral ligament close to the phalangeal attachment, most commonly at the inferolateral aspect of the joint (Fig. 13). On US, most plantar plate tears are seen as discrete partial or full thickness hypoechoic defects in the plate substance^(13,14). Flattening or attenuation may occur with plantar plate degeneration. When the plantar plate is completely torn, the flexor digitorum tendon may directly contact the metatarsal head^(13,14). In the chronic setting, reactive pericapsular fibrosis can be seen as

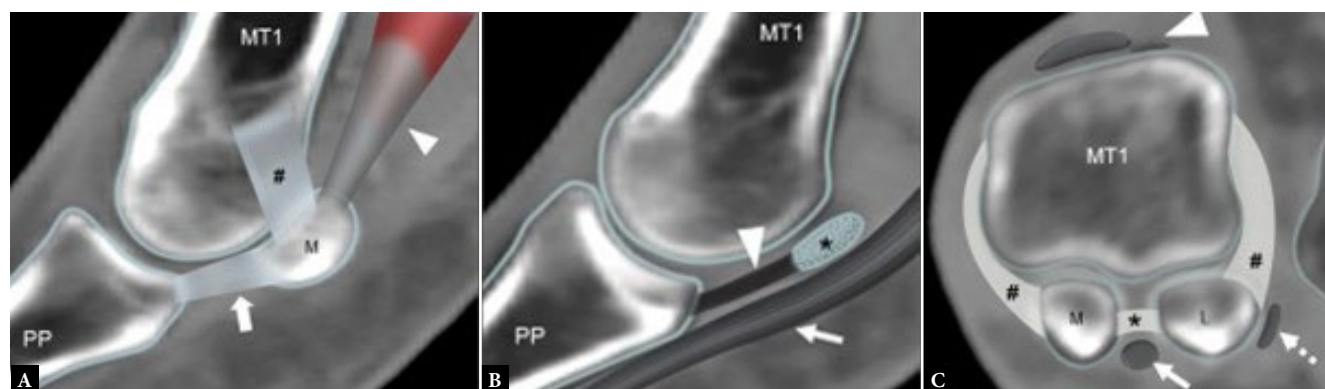


Fig. 11. Schematics of the 1st MTP joint A. Paramedian sagittal section shows the medial sesamoid bone (M) held in place by the flexor hallucis brevis tendon (arrowhead), medial metatarso-sesamoid ligament (#) and the medial sesamoid-phalangeal ligament (arrow). B. Midline sagittal section shows the plantar plate (arrowhead) attached to the intersesamoid ligament (*) and base of proximal phalanx (PP) with the overlying flexor hallucis longus tendon (arrow). C. Transverse section through the head of the 1st metatarsal bone (MT1) shows the medial (M) and lateral (L) sesamoid bones held in place by the paired medial and lateral metatarso-sesamoid ligaments (#) and the inter-sesamoid ligament (*). The flexor hallucis longus (arrow) and conjoint adductor hallucis (dotted line) tendons are also shown, as are the extensor tendons (arrowhead)

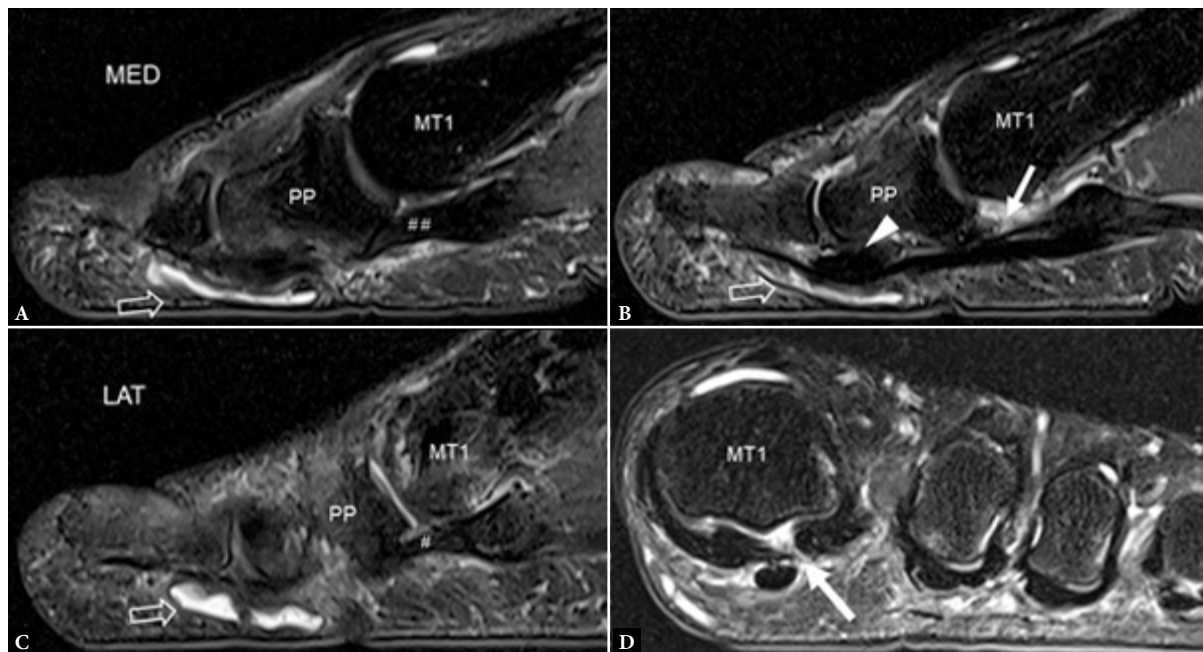


Fig. 12. 58-year-old female with forefoot pain. T2W fat-suppressed sagittal images through the A. medial, B. mid-line, and C. lateral aspects of the big toe. At the 1st MTP joint, the Index medial (##) and lateral (#) metatarso-sesamoid ligaments are intact with a complete tear of the attenuated plantar plate (arrow). At the interphalangeal joint, there is a degenerative thickened plantar plate (arrowhead) with an overlying mildly distended adventitial bursa (open arrow). D. T2W fat-suppressed coronal image also shows a tear of the inter-sesamoid ligament (arrow). MT1, 1st metatarsal bone, PP, proximal phalanx

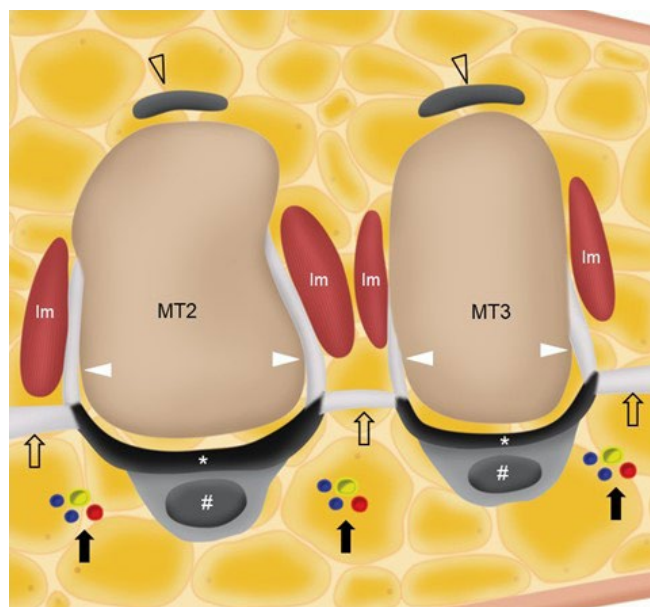


Fig. 13. Schematic coronal section of the 2nd and 3rd lesser MTP joints shows the plantar plate (*) firmly attached to paired medial and lateral accessory collateral ligaments (arrowheads). The intermetatarsal ligaments (open arrows) and digital neurovascular bundles (arrows) are shown as are the flexor (#) and extensor digitorum tendons (open arrowheads). The interosseous muscles (Im) are also shown

a non-compressible hypoechoic cuff of tissue abutting the plantar and inferolateral (or inferomedial) aspects of the MTP joint^(13,14). US should be performed in both longitudinal and transverse planes, scanning the plantar aspect of the MTP joint slowly from lateral to medial and from distal to proximal, with angling of the transducer to avoid anisotropy. Most injuries occur at the distal attachment of the

plate. Longitudinal US is best to detect and characterize tears while transverse US is useful to delineate the eccentric location of pericapsular fibrosis and to exclude subluxation of the flexor digitorum tendon. Longitudinal US during toe dorsiflexion can improve tear detection and appreciation of MTP joint subluxation⁽¹⁴⁾.

For MR imaging, T1-weighted (T1W) coronal images are usually the most helpful as routine sagittal forefoot images do not always image the plantar plate in a true sagittal plane⁽¹²⁾ (Fig. 15). Performing MRI in the prone position, with the foot in plantarflexion, results in less magic angle artifact and less movement artefact potentially facilitating assessment of the plantar plate⁽¹¹⁾. Prone positioning also leads to slight plantar shift of the interdigital soft tissues improving assessment of Morton's neuroma⁽¹⁵⁾. Dynamic US assessment during MTP joint dorsiflexion or during dorsal drawer (Lachman) testing can help assessment of plantar plate integrity and MTP joint stability. Compared with surgical findings, the pooled sensitivity (93%) of US for detecting plantar plate tears is comparable to that of MRI (89–95%), though MRI has a higher specificity (54–83%) than US (33–52%)⁽¹⁶⁾. A negative US examination makes plantar plate injury very unlikely. If US is positive or equivocal, MRI can provide more specificity as to the nature of the injury and yield a more global assessment of the MTP joint⁽¹⁷⁾.

Additional indirect MRI signs of plantar plate tear are joint effusion, subarticular BME, flexor tenosynovitis, an elongated 2nd metatarsal bone, and reparative pericapsular fibrosis while intermetatarsal bursitis and Morton's neuroma are quite common accompaniments. Pericapsular fibrosis is a useful indirect sign of chronic plantar plate tear which often mimics Morton's neuroma (i.e. 'pseudoneuroma')⁽¹¹⁾ (Fig. 16). Helpful features to distinguish between pericapsular fibrosis and Morton's neuroma are listed in Tab. 3. It is likely that as pericapsular fibrosis/plantar plate tear becomes more widely recognized, less Morton's neuromas and more chronic plantar plate tears will be diagnosed.

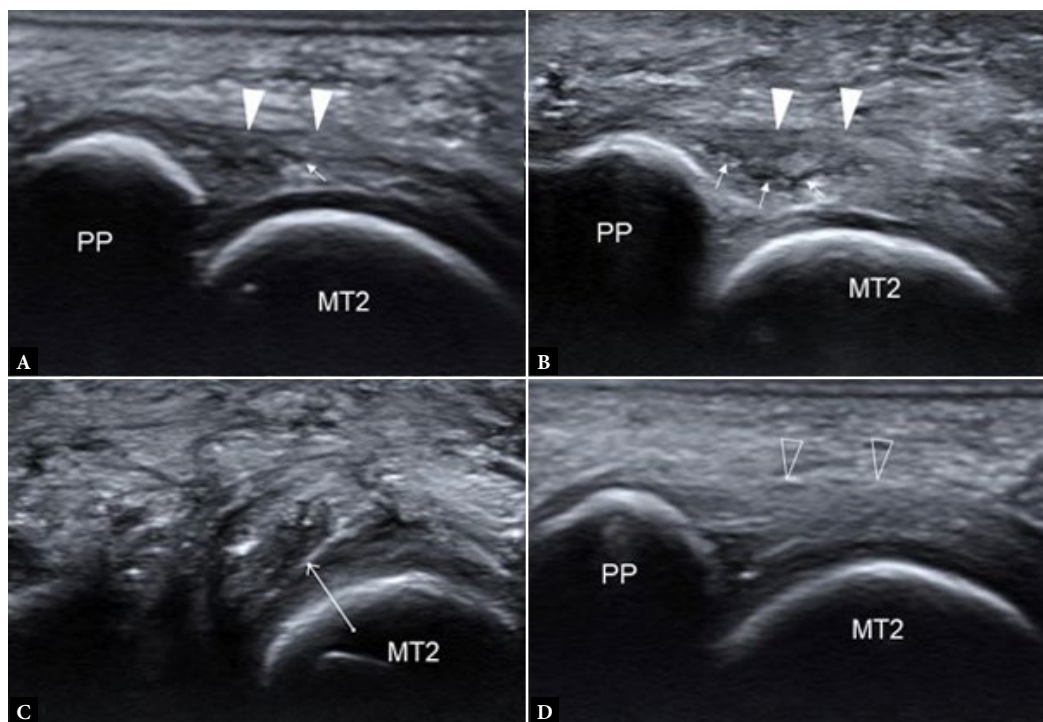


Fig. 14. 31-year-old female professional basketball player with forefoot pain. **A, B.** Consecutive longitudinal greyscale US images shows moderately thickened plantar plate (arrowheads) of the 2nd MTP joint with a long intrasubstance tear (short arrows). **C.** Transverse greyscale US image shows moderate pericapsular fibrosis (long arrow) inferolateral to the 2nd MTP joint. **D.** Longitudinal greyscale US image of the asymptomatic normal contralateral 2nd MTP joint plantar plate for comparison. (images courtesy of Dr James Linklater)

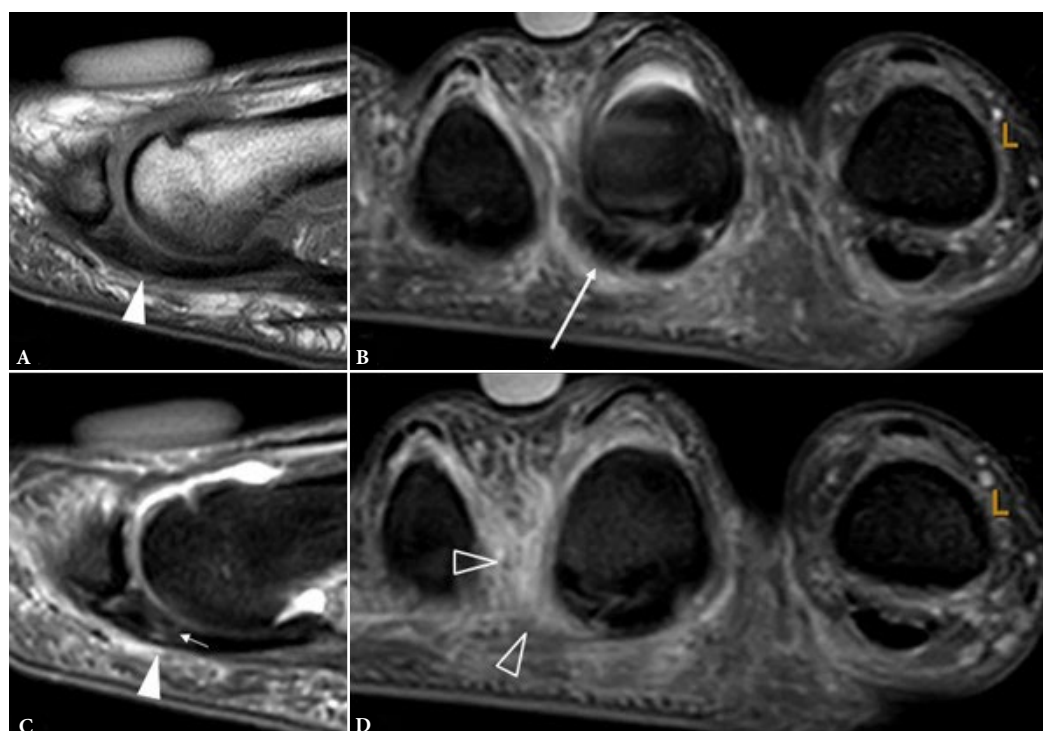


Fig. 15. Same patient as previous figure. Sagittal **A.** proton density (PD) and **B.** T2W FS images shows a moderately thickened plantar plate (arrowheads) of 2nd MTP joint with intrasubstance tear (short arrow). **C, D.** Coronal T2W fat-suppressed MR images shows moderate-severity reactive pericapsular fibrosis (long arrow) inferolateral to the 2nd MTP joint with moderate pericapsular inflammation (open arrowheads). The plantar plate tear was confirmed and treated surgically, with subsequent return to sports (images courtesy of Dr James Linklater)

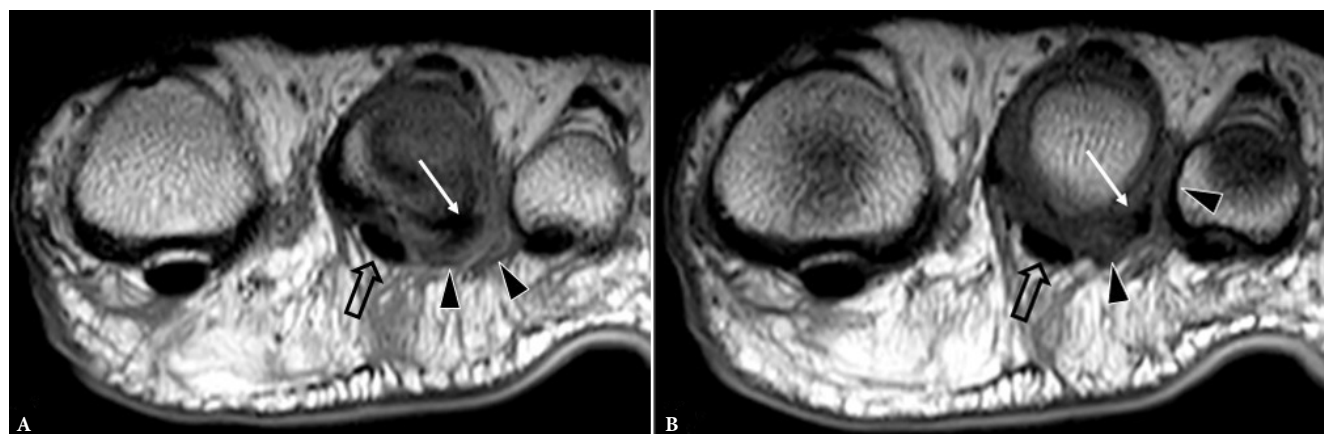


Fig. 16. 43-year-old female with forefoot pain due to 2nd MTP joint plantar plate tear. T1W coronal MR images forefoot shows severe pericapsular fibrosis (arrowheads) at the inferolateral aspect of 2nd MTP joint extending along the lateral margin of the joint. The lateral accessory collateral ligament is shown (arrow) as well as the flexor digitorum tendon (open arrow). The flexor tendon is medialized, which supports a lateral plantar plate injury

Tab. 3. Features helpful in distinguishing the pericapsular fibrosis of lesser metatarsophalangeal (MTP) plantar plate injury from the perineural fibrosis of Morton’s neuroma

	Pericapsular fibrosis	Morton’s neuroma
Location	2 nd > 3 rd MTP	3 rd > 2 nd intermetatarsal space
Shape of fibrotic mass	Crescent-shaped	Roundish or ovoid ± ginkgo leaf shape on side-to side compression
Base of fibrotic mass	Abuts inferolateral (or inferomedial) aspect of affected MTP joint over a broad area	Located centrally in intermetatarsal space ± contacts but does not envelope MTP joint capsule
Continuity with common interdigital nerve	No continuity	Continuity may be visible
Tenderness	Maximum over MTP joint region	Maximum over intermetatarsal area
Mulder maneuver	Negative (no displacement of fibrotic mass)	± Positive (fibrotic mass displaces inferiorly)
Plantar plate integrity	Additional 1 ^o or 2 ^o features of plantar plate degeneration / tear usually present	MTP joint usually normal
MTP joint stability (Hamilton-Thompson test)	± Unstable	Stable

Bursitis

Intermetatarsal bursitis. The intermetatarsal bursae have a synovial lining and are located in the superior intermetatarsal space, dorsal to the intermetatarsal ligament⁽¹⁸⁾. Bursal enlargement of >3 mm in the axial plane is considered significant. Intermetatarsal bursitis may be seen on MRI in early RA before clinical joint swelling in patients with clinically suspected arthralgia⁽¹⁹⁾ (Fig. 17).

Adventitial bursitis can occur at any pressure point (Fig. 12) and is often seen alongside the 1st and 5th metatarsal heads. If inferior to the metatarsal heads, it is known as submetatarsal bursitis (Fig. 18). Adventitial bursae have no synovial lining. Active bursitis is seen on MRI and US as a sharply demarcated area with variable soft tissue inflammation, hyperemia, and contrast enhancement. Chronic inactive bursitis can appear like reactive fibrosis with no discernible fluid and localized soft tissue thickening, low in signal on both T1W and T2-weighted (T2W) imaging. Submetatarsal bursitis is more common in RA patients than in patients with other arthritides or healthy volunteers, and tends to occur plantar deep to the 1st and 5th metatarsal heads⁽¹⁸⁾.

Diffuse submetatarsal alteration (DSMA) or metatarsal fat pad atrophy is a common cause of metatarsalgia. It is seen plantar to

the metatarsal heads, with thinning and poorly defined edema of the metatarsal fat pads either on US or MRI examination with or without diffuse contrast enhancement⁽¹⁸⁾ (Fig. 19). Hyperemia is not usually a feature. No discrete bursitis is present. Any of the metatarsal heads may be affected. Occurrence under the first and fifth metatarsal heads is most likely due to mechanical loading. In rheumatoid arthritis, DSMA occurs mainly under the 2nd, 3rd, and 4th metatarsal heads⁽¹⁸⁾. Metatarsal fat pad atrophy is currently a subjective assessment, based on a general perception of submetatarsal tissue thickness, as no reliable age-related normative data are available (Fig. 19).

Soft tissue masses

Soft tissue masses in the mid- and forefoot region are nearly always benign. The most frequently encountered masses are ganglion cyst, Morton’s neuroma, gouty tophus, plantar fibroma, leiomyoma, nerve sheath tumor, lipoma, vascular malformation, tenosynovial giant cell tumor (Ts-GCT), and foreign body granuloma⁽²⁰⁾. In most instances, US enables an accurate assessment and characterization based on imaging findings alone, without the need for percutaneous biopsy or additional imaging. If histological confirmation is required prior to definitive treatment as, for example, in most cases of Ts-GCT, percutaneous biopsy is undertaken. Additional imaging

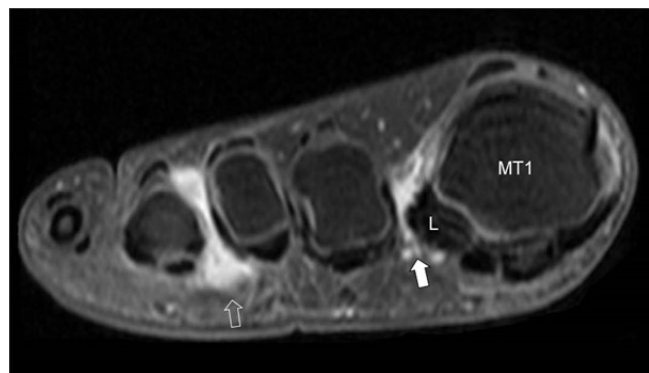


Fig. 17. Coronal gadolinium-enhanced T1W FS MR image at the level of the MTP joints of a patient with early arthritis. There is enhancement of the intermetatarsal bursae in the 1st (arrow) and 3rd (open arrow) web spaces. The lateral sesamoid bone (L) and 1st metatarsal base (MT1) is rotated such that impingement between this sesamoid bone and the 2nd metatarsal bone may be leading to inflammation of the 1st intermetatarsal bursa



Fig. 18. Transverse color Doppler US image plantar aspect of foot at the level of the 1st metatarsophalangeal joint shows a large well-demarcated hypoechoic area (*) in the subcutaneous tissue, consistent with a distended sub-metatarsal bursa. There is no hyperemia

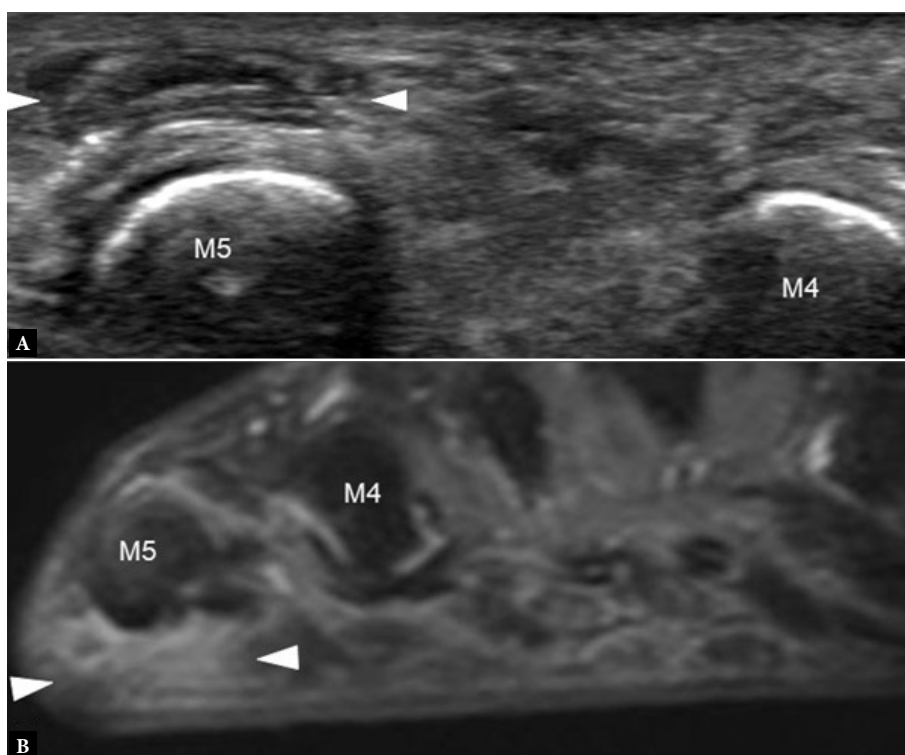


Fig. 19. 36-year-old female with lateral forefoot pain. **A.** Transverse greyscale US image shows localized metatarsal fat pad atrophy with thinning of the sub-metatarsal tissues and edema plantar to the 5th metatarsal head (M5). No discrete sub-metatarsal bursitis is present. M4, 4th metatarsal head. **B.** Corresponding T2W FS coronal image shows similar features (arrowheads) to figure A

with MRI is usually very helpful if the mass is large or deep extension cannot be fully defined on US examination.

Morton's neuroma

Rather than being a true neuroma, Morton's neuroma is a reactive-type fibrous mass in and around a plantar common digital nerve, usually occurring where the common interdigital nerve divides into its medial and lateral digital branches and leading to a focal increase

in nerve size. These nerves are located plantar to the intermetatarsal ligament (Fig. 13), which is helpful when distinguishing Morton's neuroma from intermetatarsal bursitis⁽¹⁸⁾.

Morton's neuroma is mostly seen in middle-aged women, and is possibly related to mechanical loading from high-heeled shoes. Patients typically have intermetatarsal head pain or numbness radiating to the adjacent toes. US, which can be performed from either the dorsal or plantar side, allows close clinical correlation and dynamic assessment⁽¹³⁾. Pressure with the thumb from the dorsal aspect of the

forefoot as well as the squeeze test (Mulder's maneuver) help move the hypochoic neuroma towards the plantar placed transducer⁽¹³⁾ (Fig. 20). This displacement of the neuroma may be accompanied by a palpable, or even audible, click. On longitudinal US, Morton's neuroma is seen as a normal fibrillar echogenic common interdigital nerve coursing into a focal heterogeneous hypochoic mass about 14 mm in length (range, 9.0–24.0 mm) containing a more central echogenic area, about 7.5 mm in length⁽²¹⁾. The central echogenic area more closely approximates the size of the actual neuroma histologically with the surrounding hypochoic area representing scar tissue⁽²¹⁾. On histology, the resected neuroma will comprise a "neuroma-bursal complex" consisting of the thickened degenerated nerve, fibrotic perineurium, tangled vessels, and scarred/ thickened bursa⁽²¹⁾. A neuroma >5 mm in transverse dimension is more likely to be symptomatic⁽¹³⁾.

On MRI, Morton's neuroma is seen as a rounded to spindle-shaped T1-intermediate signal, T2-hypointense mass in the inferior intermetatarsal space, either with or without contrast enhancement. Visible continuity with the plantar digital nerve ('rat's tail sign') also improves diagnostic confidence. In contrast, intermetatarsal bursitis is more cyst-like, with rim enhancement in the superior intermetatarsal space (Fig. 17)⁽²²⁾. Both US and MRI have comparable high sensitivity for diagnosing Morton's neuroma, with US being more cost-effective⁽²³⁾.

Ganglion cyst

A ganglion cyst is connected to a joint or, less commonly, a tendon sheath. It contains synovial fluid, though the cyst itself has no syno-

vial lining. Visualizing a deep connection, which may be thin and serpiginous, enables a more definitive diagnosis and is helpful for surgical excision (Fig. 21). Occasionally, only a suggestion of a tract pointing towards the joint of origin is apparent. On MRI, a ganglion cyst is seen as a demarcated mass with a high signal intensity on fluid-sensitive sequences, which may be multilobular with septae, and display peripheral enhancement after intravenous gadolinium administration.

US is the method of choice for examining suspected ganglion cysts and shows a well-defined anechoic lesion, occasionally multilocular, and usually non-compressible (Fig. 21). Occasionally, echogenic colloid aggregates suspended within the myxoid cyst fluid may be visible. Emptying or reducing the size of the cyst by US-guided aspiration with a large bore needle and intra-cystic corticosteroid injection is sometimes helpful. Some cysts may be too viscous to aspirate. In the absence of intracystic suspensions, it is not possible to gauge cyst content viscosity. A smaller, and usually less symptomatic, cyst remnant often persists following aspiration⁽²⁴⁾.

Plantar fibromatosis (Ledderhose disease)

Plantar fibromatosis is a benign condition with focal nodular fibrous enlargement of the plantar aponeurosis (i.e. plantar fibroma). Classically, a nodule is felt by the patient at the medial side of the middle one-third of the sole. US shows a typical uniform hypochoic fusiform thickening in continuity with the plantar fascia, which may be multifocal in the same foot in one-quarter and bilateral in one-third of patients^(25,26) (Fig. 22). It can be differentiated from the much less common plantar fascial tears, which show focal reparative fibrosis with

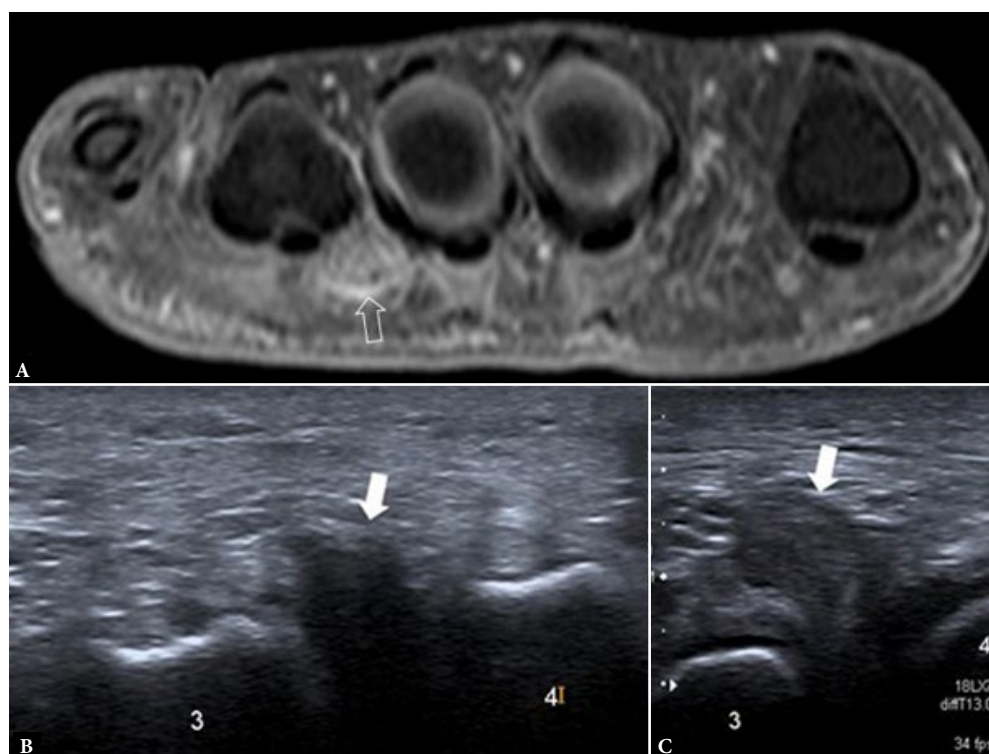


Fig. 20. Morton's neuroma in two different patients. **A.** Coronal gadolinium-enhanced T1W TSE fat-suppressed image shows inhomogeneous enhancement of a rounded mass (open arrow) on the plantar aspect of the third webspace, consistent with a Morton's neuroma. **B.** On greyscale transverse US image of the third webspace, a hypochoic mass is seen (arrow), which **C.** becomes more prominent using the squeeze test

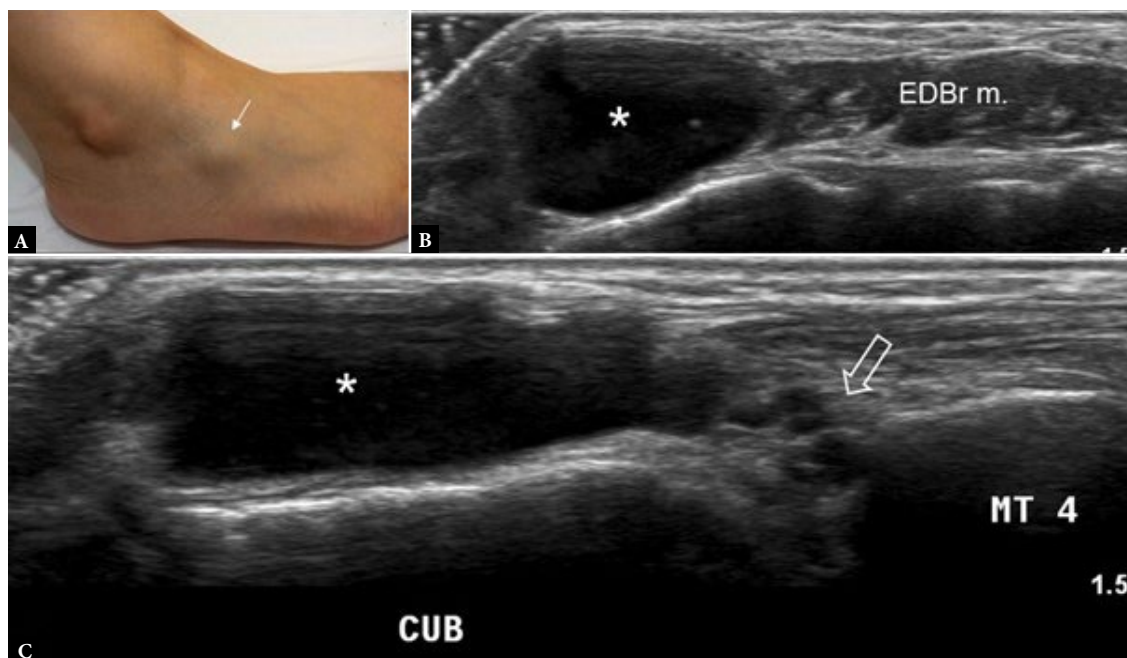


Fig. 21. A. Clinical photo of the lateral aspect of the midfoot in a 48-year-old female with non-painful mass (arrow). B. Transverse and C. longitudinal greyscale US images of the midfoot shows a medium-sized ganglion (*) arising by short track (open arrow) from the cuboid (CUB): 4th metatarsal joint (MT 4) articulation. The ganglion lies lateral to the extensor digitorum brevis muscle (EDBr m.)

or without plantar fascial discontinuity at a site of previous injury, or the more common plantar fasciitis, which is located at the calcaneal insertion. Plantar fibromas can also be seen on MRI (Fig. 23), though US examination alone is generally satisfactory. On MRI, plantar fibromas are seen as small to medium-sized fusiform-shaped nodule or clustered nodules attached to and extending along the plantar aponeurosis ('fascial tail sign'), usually the medial cord. T2 hyperintense (relative to muscle) lesions with avid contrast enhancement tend to be actively growing lesions, containing proliferative fibroblastic tissue, that are more responsive to electron beam irradiation therapy, while T2 isointense or hypointense lesions with poor enhancement tend to be quiescent lesions, containing mature collagenous tissue⁽²⁷⁾.

Foreign body granuloma

This entity usually occurs in the subcutaneous fat on the plantar aspect of the foot. The patient often recalls a history of penetrating trauma. Radiopaque foreign bodies, such as metal and large pieces of glass, can be detected on radiographs. US is the preferred investigation to detect radiolucent foreign bodies, such as wood, plastic, or small glass splinters. US also allows the location of the foreign body to be precisely defined, and detects injury to structures such as tendons, nerves, and vessels⁽²⁸⁾. All foreign bodies are echogenic⁽²⁸⁾. Smooth, flat surfaces will lead to a hypoechoic, 'dirty' acoustic shadowing, while irregular, curved surfaces will lead to echogenic, 'clean' shadowing⁽²⁸⁾. Often, the US is performed weeks or months following initial penetrating injury. In such instances, US reveals a hypoechoic halo of granulation tissue on greyscale imaging, either with or without hyperemia, close to or encasing the hyperechoic foreign body on Doppler imaging (Fig. 24). The size of the hypoechoic halo will vary depending on the intensity of foreign body reaction induced. Such reactions may occasionally be seen after 24 hours⁽²⁸⁾. Abscess is infrequently present.

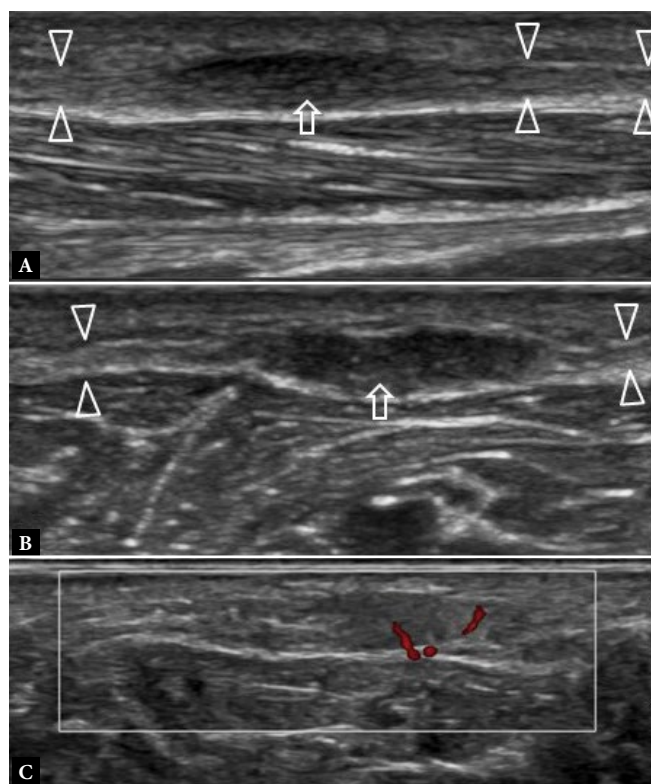


Fig. 22. 63-year-old female with a plantar foot mass for one year, painful on weight-bearing. A. Longitudinal and B. transverse greyscale US images show a medium-sized fusiform-shaped plantar fibroma (arrow) arising from the central band of the plantar fascia (arrowheads). C. Color Doppler US image shows mild hyperemia of plantar fibroma. This is an unusual feature which may reflect a more active lesion containing proliferative fibroblastic tissue, similar to contrast enhancement seen on MR examinations

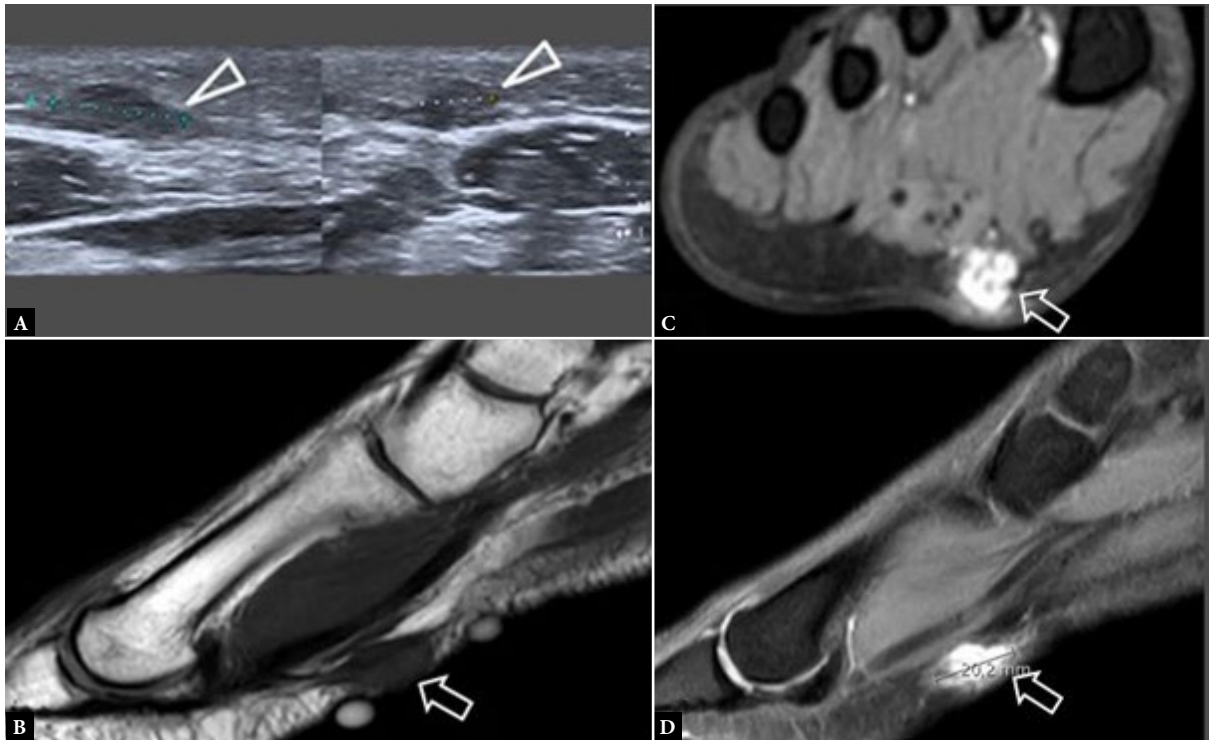


Fig. 23. 21-year-old male with a palpable mass medioplantar aspect of foot. **A.** On greyscale US image, the mass (arrowheads) is hyperechoic (to muscle) and connected to the plantar aponeurosis consistent with a plantar fibroma (Ledderhose disease). **B.** Sagittal T1-weighted (**C**) coronal and (**D**) sagittal T1 fat-suppressed contrast-enhanced images show the lesion to be avidly enhancing (arrows) suggestive of an active lesion containing proliferative fibroblastic tissue with mild surrounding inflammation

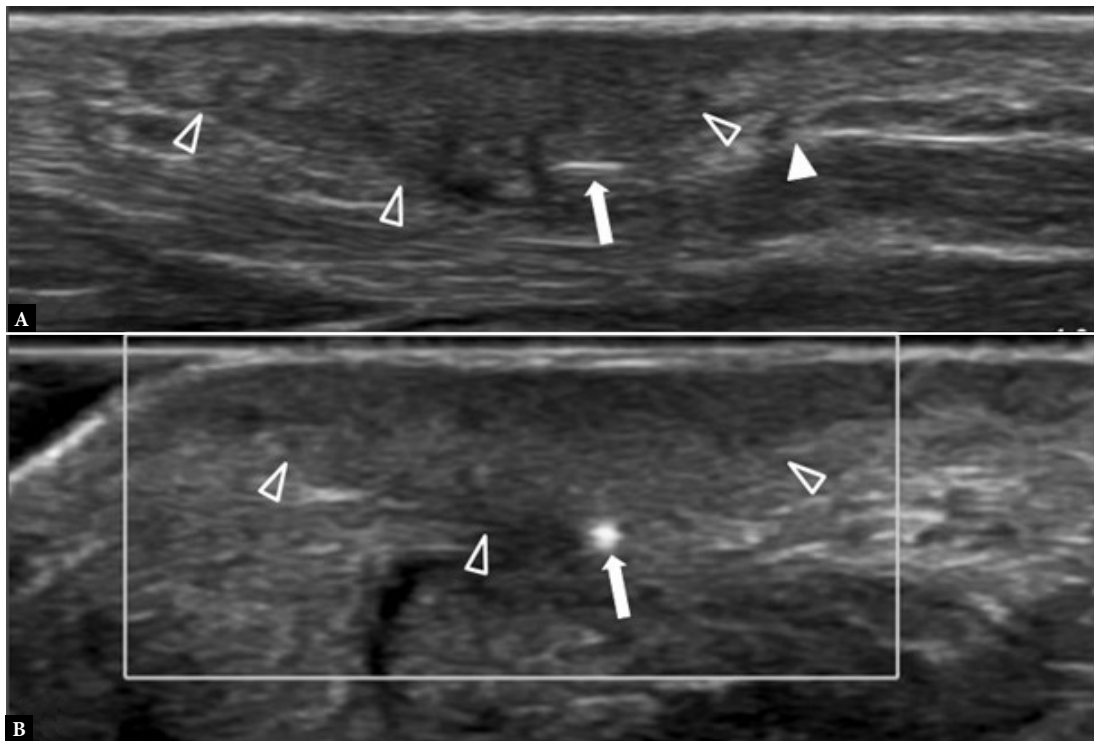


Fig. 24. 72-year-old female with tree branch puncture injury to sole four months previously, who subsequently developed a pyoderma granuloma-like skin wound at the puncture site. **A.** Longitudinal greyscale US image of sole show a quite well-defined area of subcutaneous fibrosis (open arrowheads) extending down to the level of the plantar aponeurosis (arrowhead). At the deeper margin of this fibrotic area is a linear echogenic structure (arrow), consistent with a small wood splinter. **B.** Transverse color Doppler US image shows that the fibrotic-type tissue (arrowheads) was not hyperemic. The area of fibrosis and wood foreign body (arrow) were removed at subsequent surgery to good effect

Leiomyoma

Two-thirds of leiomyomas (or angioleiomyomas) occur in the lower leg, ankle, or foot region. This is a benign solitary smooth muscle tumor that mostly occurs in the subcutaneous tissues. Most are <2 cm in diameter and occur close to neurovascular bundles⁽²⁹⁾. On US, they are well-defined, homogeneously hypoechoic, or ovoid, with a smooth margin, even though no discernible capsule is seen. About half of leiomyomas will have small hypoechoic protrusions at one or both ends of the mass, most likely due to extension along the vessel of origin⁽²⁹⁾. Mild to moderate posterior enhancement is usually seen⁽²⁹⁾. Most tend to be moderately hypervascular, occasionally with peripheral vascular convergence (Fig. 25). Many of these features can also be seen in small subcutaneous peripheral nerve sheath tumors arising from small subcutaneous nerves and, as such, do not have a visible neural tail. Consequently, the distinction between leiomyoma and nerve sheath tumor is often difficult.

Joint disorders

Osteoarthritis

Osteoarthritis may affect any joint in the mid- to forefoot, but it most commonly involves the joints of the medial longitudinal arch. The medial column, which is composed of the 1st MTP joint, or middle column, which comprises the 2nd and 3rd MTP joints, are usually affected more than the lateral column, which includes the 4th and 5th

MTP joints⁽³⁰⁾. Patients present with pain aggravated by prolonged weight-bearing. Radiography is the first line of investigation. US is usually undertaken to establish osteoarthritis as the likely cause of dorsal midfoot pain and swelling. Dorsal foot swelling in such instances is typically caused by hypertrophic dorsal osteophytes and capsular/soft tissue swelling, though paraarticular ganglia are also common. US reveals joint space narrowing with marginal osteophytosis, capsular thickening, and mild surrounding soft tissue swelling, possibly with hyperemia on Doppler imaging (Fig. 26)⁽³⁰⁾. As the curvature of the articular surfaces and marginal osteophytosis limits accurate US assessment of joint space narrowing, radiographic correlation is useful in this regard. If surgery is considered, CT optimizes delineation of osseous anatomy, disease extent, and severity, as well as alignment. Cone beam CT is a small footprint, self-shielded device, producing high-quality localized CT images of the mid- and forefoot, and is a useful emerging imaging modality for foot osteoarthritis, not least that the examination can be obtained in the weight-bearing position⁽³⁰⁾. MRI is advantageous in showing subchondral BME, which is moderately associated with pain with or without focal articular cartilage defects. MRI, however, is usually not required to investigate suspected mid- and forefoot osteoarthritis.

Gout

Gravity and the relatively colder temperatures of the mid- and forefoot encourage uric acid crystal deposition. This deposition mainly occurs in periarticular tissues and ligamentous insertions. Intratendinous or peritendinous deposition is also common (Fig. 27). The

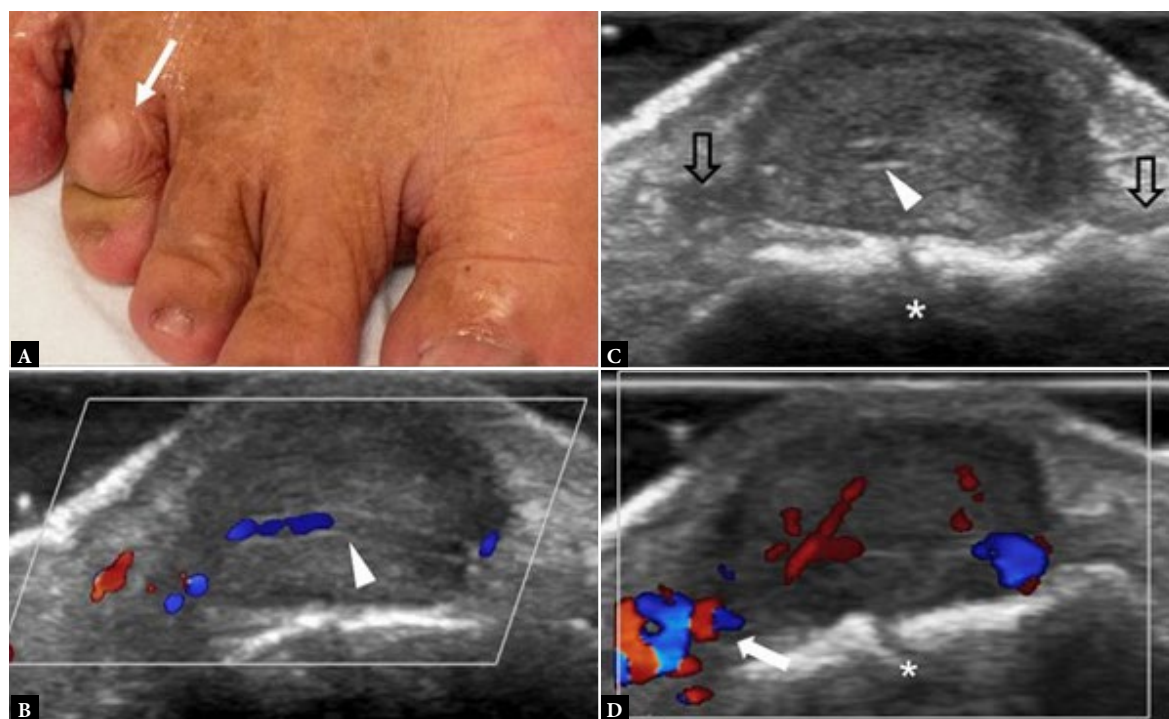


Fig. 25. A. Clinical photo of 72-year-old female with an occasionally painful mass (arrow) on the dorsum of the 4th toe for one year. B. Longitudinal greyscale and (C, D) color Doppler US images show a small well-defined ovoid subcutaneous mass on the dorsum of the toe overlying the distal interphalangeal joint (*). There are small hypoechoic protrusions proximally and distally (open arrows). The mass seems to arise from the medial digital artery which coursed through the center of the mass (arrowheads). There is an impression of vascular convergence (open arrow) at the proximal aspect of the moderately hyperechoic mass. No deep extension was evident. Leiomyoma was considered the most likely diagnosis. Less likely differential diagnoses included Kimura's disease, giant cell tumor of tendon sheath, and nerve sheath tumor. Excisional biopsy confirmed leiomyoma

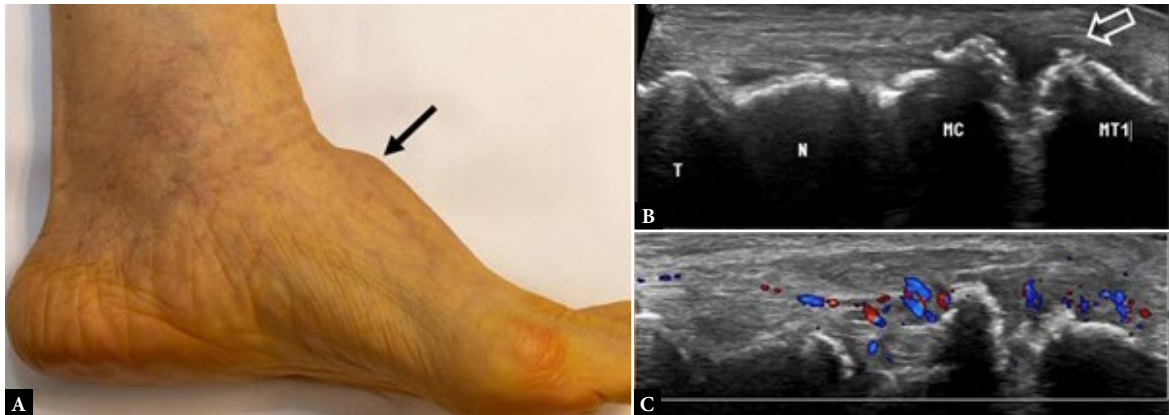


Fig. 26. A. Clinical photograph of a 73-year-old female with painful dorsal foot swelling (arrow) for 10 years. B. Longitudinal greyscale US image of the dorsum of the midfoot shows severe osteoarthritis with dorsal marginal osteophytosis and capsular swelling (open arrow), particularly between the 1st metatarsal (MT1) bone and the medial Index cuneiform (MC) bone, and, less so, between the medial cuneiform and navicular (N) bones. The joint between the navicular bone and the talus (T) is preserved. C. Longitudinal color Doppler US at the same location shows moderate capsular hyperemia

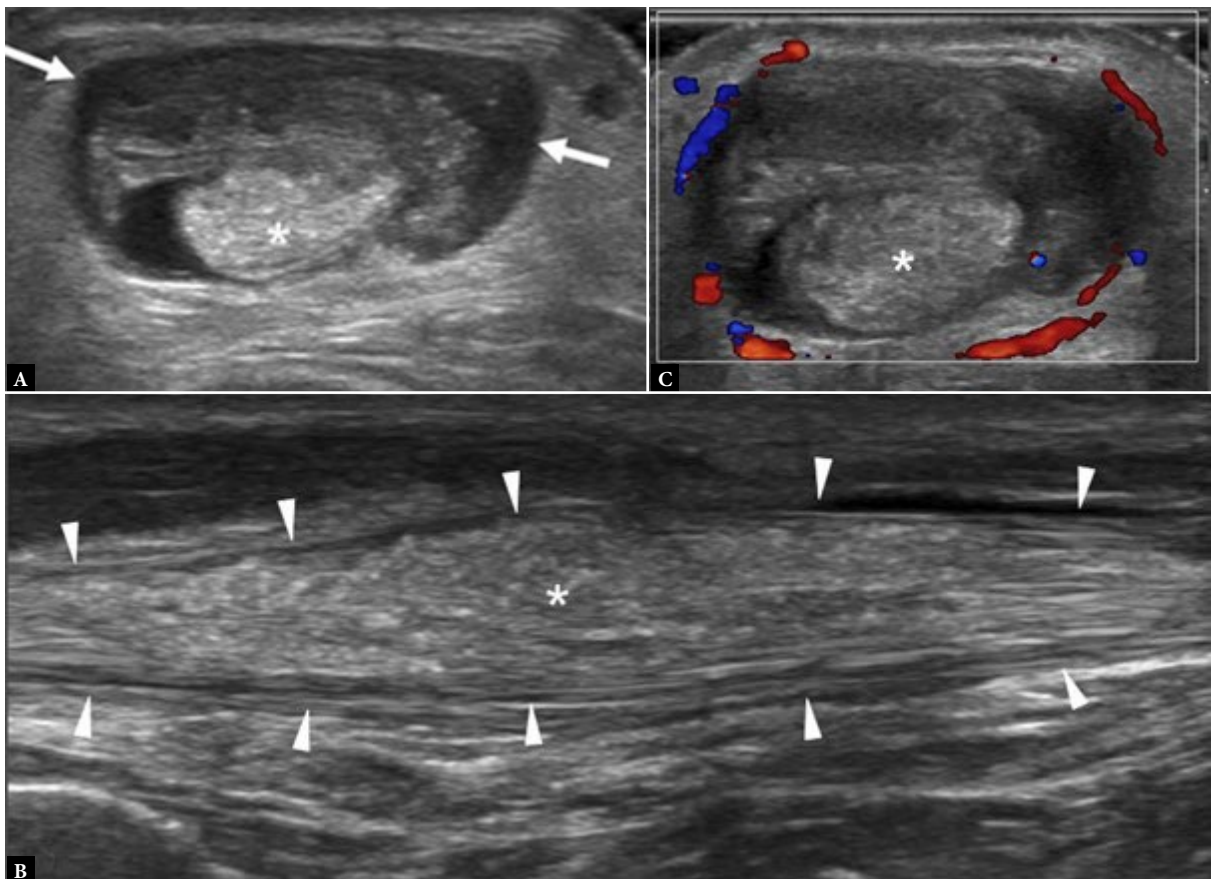


Fig. 27. 75-year-old man with known gout and dorsal mid-foot swelling for one year. A. Transverse and B. longitudinal greyscale US images shows speckled gouty crystal deposition (*) expanding the tibialis anterior tendon (arrowheads) and its distended tendon sheath (arrow). C. Transverse color Doppler US image shows moderate hyperemia around the distended tendon sheath

first MTP joint is the most affected. Patients may present acutely with a painful joint similar to septic arthritis, or chronically with an intermittently painful mass or an enlarged joint due to gouty tophi. A diagnosis of gouty arthritis/gouty tophi can usually be adequately established with radiographs and US. There is usually little benefit to performing MRI examination. Dual energy CT is helpful to es-

tablish the presence of uric acid accumulations, though it is falsely negative in gouty arthritis without uric acid accumulation.

Calcium pyrophosphate deposition (CPPD) can also occur in the foot. The presentation is similar to gout, though tophi tend to be less prevalent, and crystal deposition occurs in the mid-zone articu-

lar cartilage layer, as opposed to the cartilage surface, though such delineation is generally not feasible in the thin articular cartilage of the foot.

Hallux valgus

Hallux valgus is excessive adduction at the first MTP joint. This diagnosis is made clinically, with supportive radiographs⁽³¹⁾. US is usually not necessary, though it may reveal osteoarthritis of the first MTP joint. MRI is usually not indicated. The normal hallux angle is 8–12°⁽³¹⁾. Adventitious bursitis is a relatively uncommon complication of hallux valgus that can be assessed by US.

Pes planus

Pes planus, or flatfoot, results from variable collapse of the medial longitudinal arch. This can be associated with posterior tibialis tendinosis either at its insertion or along the course of the posterior tib-

ialis tendon (Fig. 28). Tendinosis and tendon tears can be evaluated well with US, as can the presence of an often accompanying accessory navicular bone or cornuate configuration to the medial pole of the navicular bone. MRI allows a more comprehensive assessment of navicular configuration, medial longitudinal arch flattening, talar head support, heel valgus, sub-talar and sub-fibular impingement, as well as reactive ligamentous thickening and tears.

Arthritides

Rheumatoid arthritis (RA)

Synovitis and tenosynovitis

RA, which is primarily a disease of the synovium, usually affects the small joints of the wrists, hands, and feet. Over the last two decades, with more effective medication, emphasis has shifted towards early

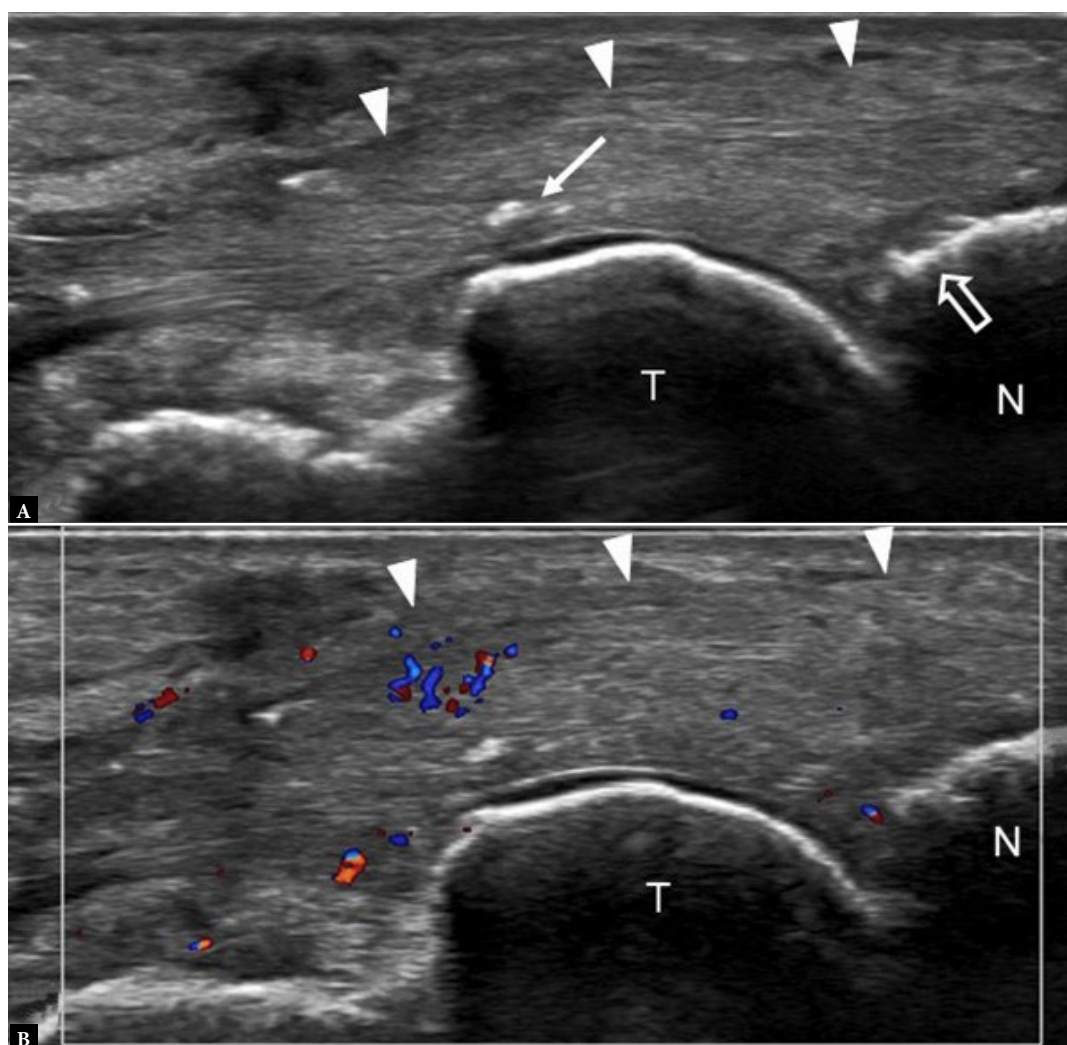


Fig. 28. 59-year-old man with painful midfoot medially. **A.** Longitudinal greyscale US image shows thickened posterior tibialis tendon (arrowheads) with mild dystrophic calcification (arrow) at and close to the navicular bone (N) insertion. Mild cortical irregularity (open arrow) of the navicular bone insertional area is also present. No tendon tear is seen. T, talar head. **B.** Mild tendon hyperemia is present. Appearances indicate moderate-severity posterior tibialis insertional tendinosis

disease detection, early treatment, and minimization of joint damage. Both US and MRI can detect subclinical synovitis and tenosynovitis, while MRI can, in addition, detect BME ('osteitis') (Fig. 29, Fig. 30). In patients with undifferentiated arthritis (UA), MRI-detected inflammation predicts RA development. The European League Against Rheumatism (EULAR) advocates using MRI in the diagnostic process^(32,33). MR parameters used in the RA-MRI scoring method (RAMRIS) include BME, synovitis, tenosynovitis, and erosions⁽³⁴⁾. To reduce costs and optimize image resolution, only the most symptomatic joint area, rather than MRI of both wrists, hands, ankles, and feet, is undertaken⁽³⁵⁾. MRI of early RA is facilitated by using a short, modified Dixon protocol instead of gadolinium-enhanced T1W FS MRI-sequences⁽³⁶⁾.

US is less sensitive than MRI in the detection of early synovitis and tenosynovitis⁽³⁷⁾. Tenosynovitis close to the MTP joints is probably a primary synovitis feature rather secondary to MTP synovitis, as anatomic study of the synovial sheaths shows the presence of synovial cells in both the extensor and flexor tendons at the MTP joint level⁽³⁸⁾.

Clinical disease activity score (DAS28) is one of the best measures to determine RA disease activity, with a persistently high score associated with an increased likelihood of progressive joint damage, even in clinically well patients⁽³⁹⁾. There is a discordance between clinical and US scores for assessing disease activity, and no consensus on how many joints to count during US assessment, limiting the use of US for assessing disease activity in RA^(40,41). US-guided injection is used to treat joints not responding to systemic therapy.

Tenosynovitis

Very early changes of tenosynovitis are difficult to detect. However, tenosynovitis with synovial hypertrophy and tendon sheath fluid can be readily detected with US. The flexor and extensor tendons at the MTP joint level are often involved in RA. Overuse and mechanical loading may cause tenosynovitis in non-RA patients at typical locations.

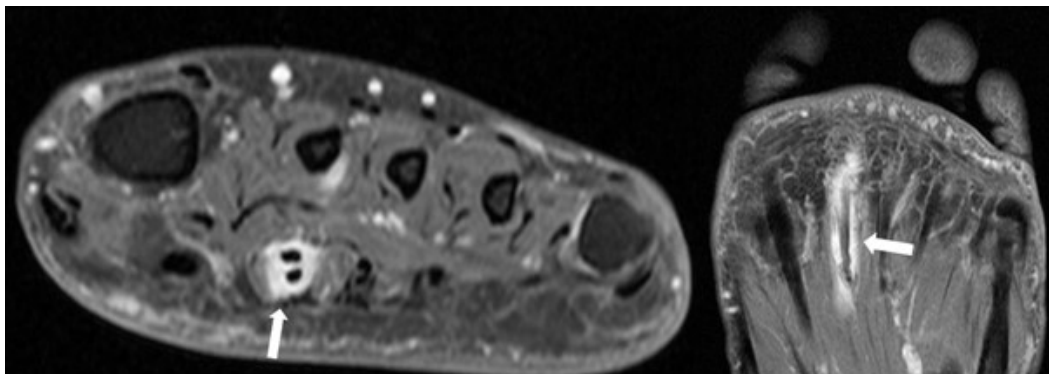


Fig. 29. A. Coronal and B. axial gadolinium-enhanced T1W fat-suppressed MR images of forefoot in a patient with early arthritis shows flexor tenosynovitis (arrows) of the second digit tendons. Mid- and forefoot tenosynovitis is a relevant parameter in early rheumatoid arthritis

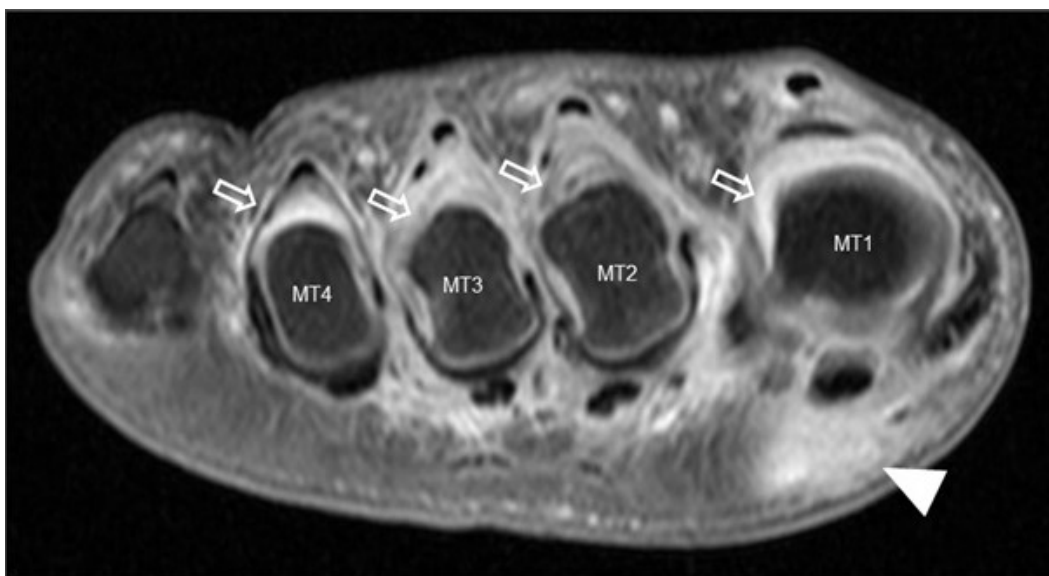


Fig. 30. Gadolinium-enhanced coronal T1W fat-suppressed MR image at the level of the MTP joints in a patient with early arthritis shows moderate synovitis (arrows) of the 1st to 4th MTP joints as well as flexor and extensor tenosynovitis. In addition, there is diffuse submetatarsal alteration (arrowhead) without discrete bursitis on the plantar aspect of the 1st MTP joint. MT1–MT4, 1st to 4th metatarsal heads

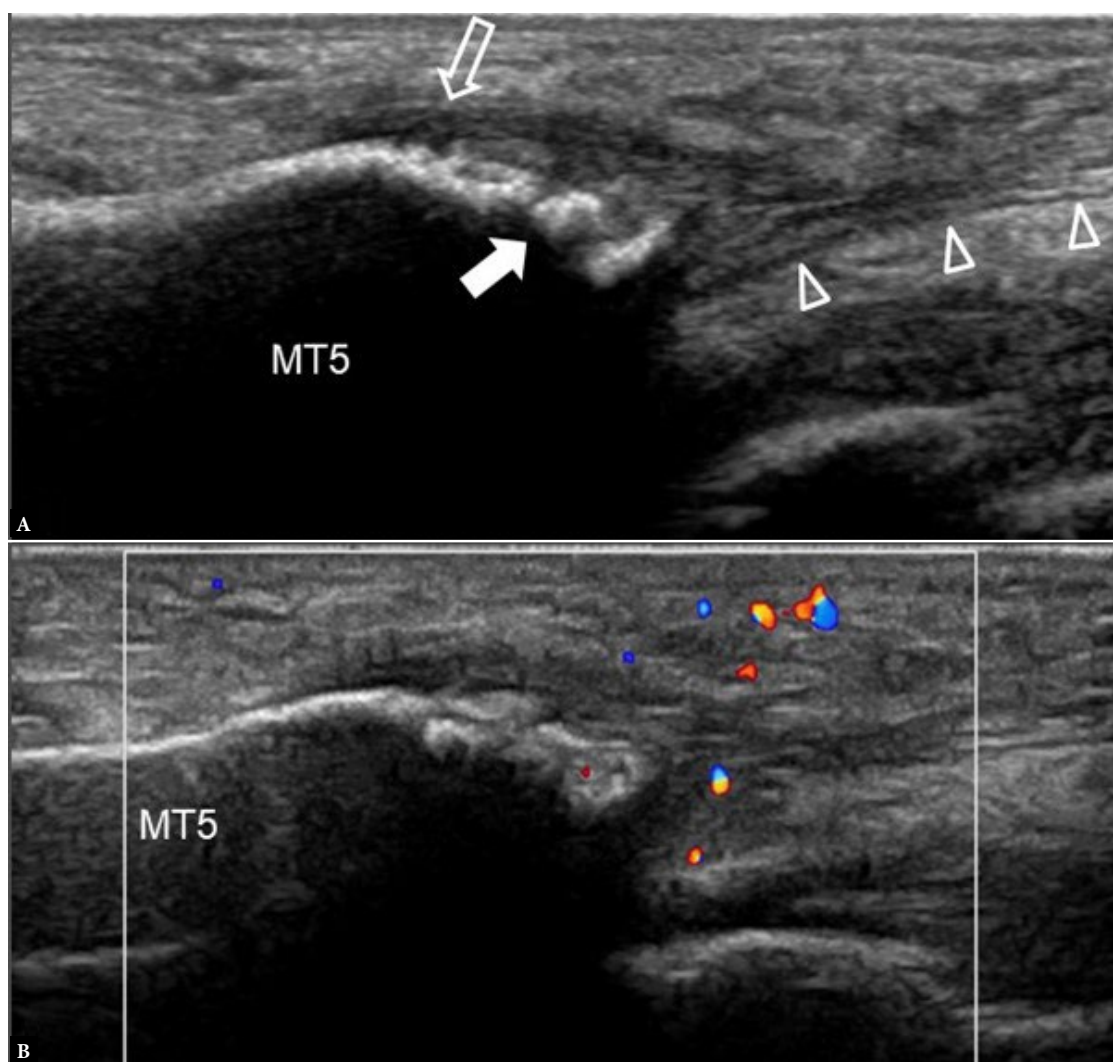


Fig. 31. 57-year-old female with unilateral lateral foot pain for several months. (A) Longitudinal greyscale US image shows moderate cortical hyperostosis (arrow) of the 5th metatarsal (MT5) base at the insertion of the lateral band plantar fascia (arrowheads). The more lateral insertion of peroneus brevis tendon (open arrow) is also shown. (B) Longitudinal color Doppler US image shows moderate localized hyperemia. Appearances are compatible with enthesitis as a feature of peripheral spondyloarthropathy. Subsequent MRI revealed inflammatory sacroiliitis due to ankylosing spondylitis

Enthesitis

Tendinous, ligamentous, or fascial insertion into bone can show thickening and hyperemia secondary to mechanical overloading or a systemic disease (e.g. spondyloarthritis, such as psoriatic arthritis). More common examples are the peroneus brevis tendon insertion and lateral band plantar fascial insertion to the 5th metatarsal base (Fig. 31) as well as the posterior tibialis tendon insertion into the medial pole of the navicular bone. When evaluating such structures, the examiner should use minimal transducer pressure during color Doppler assessment to optimize the detection of tissue hyperemia (Fig. 28, Fig. 31).

Summary

This review outlines the imaging appearances of the most common mid- and forefoot pathologies. Following radiography, high-resolution US is the examination of choice to evaluate the mid- and

forefoot. In most instances, an adequate explanation for symptoms can be found. MRI or CT may be helpful when symptoms cannot be fully explained, or the pathology cannot be fully assessed, by US examination.

Conflict of interest

The authors do not report any financial or personal connections with other persons or organizations which might negatively affect the contents of this publication and/or claim authorship rights to this publication.

Author contributions

Original concept of study: MR, JFG. Writing of manuscript: MR, JFG. Final approval of manuscript: MR, JFG. Collection, recording and/or compilation of data: MR, JFG. Critical review of manuscript: MR, JFG.

References

- Hulstaert T, Shahabpour M, Probyn S, Lenchik L, Simons P, Vanheste R *et al.*: Forefoot pain in the lesser toes: anatomical considerations and magnetic resonance imaging findings. *Can Assoc Radiol J* 2019; 70: 408–415. doi: 10.1016/j.carj.2019.06.010.
- Mandell JC, Khurana B, Smith SE: Stress fractures of the foot and ankle, part 1: biomechanics of bone and principles of imaging and treatment. *Skeletal Radiol* 2017a; 46: 1021–1029. doi: 10.1007/s00256-017-2640-7.
- Mandell JC, Khurana B, Smith SE: Stress fractures of the foot and ankle, part 2: site-specific etiology, imaging, and treatment, and differential diagnosis. *Skeletal Radiol* 2017b; 46: 1165–1186. doi: 10.1007/s00256-017-2632-7.
- Hallinan JTPD, Statum SM, Huang BK, Bezerra HG, Garcia DAL, Bydder GM, Chung CB: High-resolution MRI of the first metatarsophalangeal joint: gross anatomy and injury characterization. *Radiographics* 2020; 40: 1107–1124. doi: 10.1148/rg.2020190145.
- Hoggett L, Nanavati N, Cowden J, Chadwick C, Blundell C, Davies H *et al.*: A new classification for Freiberg's disease. *The Foot* 2022; 51: 101901. doi: 10.1016/j.foot.2021.101901.
- Koetser ICJ, Espinosa Hernández EA, Kerkhoffs PDGMMJ, Goedegebuure S, Smithuis FF, Maas PDM: Don't miss me: midfoot sprains, a point-of-care review. *Semin Musculoskelet Radiol* 2023; 27: 245–255. doi: 10.1055/s-0043-1767766.
- Kitsukawa K, Hirano T, Niki H, Tachizawa N, Mimura H: The diagnostic accuracy of MRI to evaluate acute Lisfranc joint injuries: comparison with direct operative observations. *Foot Ankle Orthop* 2022; 7: 24730114211069080. doi: 10.1177/24730114211069080.
- Mulcahy H: Lisfranc injury: current concepts. *Radiol Clin North Am* 2018; 56: 859–876. doi: 10.1016/j.rcl.2018.06.003.
- Kim J, Ellis S, Carrino JA: Weight-bearing computed tomography of the foot and ankle – what to measure? *Foot Ankle Clin* 2023; 28: 619–640. doi: 10.1016/j.fcl.2023.04.004.
- Woodward S, Jacobson JA, Femino JE, Morag Y, Fessell DP, Dong Q: Sonographic evaluation of Lisfranc ligament injuries. *J Ultrasound Med* 2009; 28: 351–357. doi: 10.7863/jum.2009.28.3.351.
- Mann TS, Nery CAS, Baumfeld D, Fernandes EÁ: Degenerative injuries of the metatarsophalangeal plantar plate on magnetic resonance imaging: a new perspective. *Einstein (Sao Paulo)* 2022; 20: eAO6543. doi: 10.31744/einstein_journal/2022AO6543.
- Mascard E, Gaspar N, Brugieres L, Glorion C, Pannier S, Gomez-Brouchet A: Malignant tumours of the foot and ankle. *EFORT Open Rev* 2017; 2: 261–271. doi: 10.1302/2058-5241.2.160078.
- Son HM, Chai JW, Kim YH, Kim DH, Kim HJ, Seo J *et al.*: A problem-based approach in musculoskeletal ultrasonography: central metatarsalgia. *Ultrasonography* 2022; 41: 225–242. doi: 10.14366/uscg.21193.
- McCarthy CL, Thompson GV: Ultrasound findings of plantar plate tears of the lesser metatarsophalangeal joints. *Skeletal Radiol* 2021; 50: 1513–1525. doi: 10.1007/s00256-020-03708-1.
- Weishaupt D, Treiber K, Kundert HP, Zollinger H, Vienne P, Hodler J *et al.*: Morton neuroma: MR imaging in prone, supine, and upright weight-bearing body positions. *Radiology* 2003; 226: 849–856. doi: 10.1148/radiol.2263011925.
- Albright RH, Brooks BM, Chingre M, Klein EE, Weil LS Jr., Fleischer AE: Diagnostic accuracy of magnetic resonance imaging (MRI) versus dynamic ultrasound for plantar plate injuries: a systematic review and meta-analysis. *Eur J Radiol* 2022; 152: 110315. doi: 10.1016/j.ejrad.2022.110315.
- Duan X, Li L, Wei DQ, Liu M, Yu X, Xu Z *et al.*: Role of magnetic resonance imaging versus ultrasound for detection of plantar plate tear. *J Orthop Surg Res* 2017; 12: 14–22. doi: 10.1186/s13018-016-0507-6.
- Dakkak YJ, Jansen FP, De Ruiter MC, Reijnierse M, van der Helm-van Mil AHM: Rheumatoid arthritis and tenosynovitis at the metatarsophalangeal joints: an anatomic and MRI study of the forefoot tendon sheaths. *Radiology* 2020; 295: 146–154. doi: 10.1148/radiol.2020191725.
- van Dijk BT, Wouters F, van Mulligen E, Reijnierse M, van der Helm-van Mil AHM: During development of rheumatoid arthritis, intermetatarsal bursitis may occur before clinical joint swelling: a large imaging study in patients with clinically suspected arthralgia. *Rheumatology* 2022; 61: 2805–2814. doi: 10.1093/rheumatology/keab830.
- Longo V, Jacobson JA, Dong Q, Kim SM: Tumors and tumor-like abnormalities of the midfoot and forefoot. *Semin Musculoskeletal Radiol* 2016; 20: 154–66. doi: 10.1055/s-0036-1581118.
- Cohen SL, Miller TT, Ellis SJ, Roberts MM, DiCarlo EF: Sonography of Morton neuroma: what are we really looking at? *J Ultrasound Med* 2016; 35: 2191–2195. doi: 10.7863/ultra.15.11022.
- Zanetti M, Strehle JK, Zollinger H, Hodler J: Morton neuroma and fluid in the intermetatarsal bursae on MR images of 70 asymptomatic volunteers. *Radiology* 1997; 203: 516–520. doi: 10.1148/radiology.203.2.9114115.
- Bignotti B, Signori A, Sormani MP, Molfetta L, Martinoli C, Tagliafico A: Ultrasound versus magnetic resonance imaging for Morton neuroma: systematic review and meta-analysis. *Eur Radiol* 2015; 25: 2254–2262. doi: 10.1007/s00330-015-3633-3.
- Ju BL, Weber KL, Khoury V: Ultrasound-guided therapy for knee and foot ganglion cysts. *J Foot Ankle Surg* 2017; 56: 153–157. doi: 10.1053/j.jfas.2016.04.015.
- Griffith JE, Wong TY, Wong SM, Wong MW, Metreweli C: Sonography of plantar fibromatosis. *AJR Am J Roentgenol* 2002; 179: 1167–1172. doi: 10.2214/ajr.179.5.1791167.
- Cohen BE, Murthy NS, McKenzie G: Ultrasonography of plantar fibromatosis: updated case series, review of the literature, and a novel descriptive appearance termed the “Comb Sign”. *J Ultrasound Med* 2018; 37: 2725–2731. doi: 10.1002/jum.14615.
- Banks JS, Wolfson AH, Subhawong TK: T2 signal intensity as an imaging biomarker for patients with superficial fibromatoses of the hands (Dupuytren's disease) and feet (Ledderhose disease) undergoing definitive electron beam irradiation. *Skeletal Radiol* 2018; 47: 243–251. doi: 10.1007/s00256-017-2792-5.
- Boyse TD, Fessell DP, Jacobson JA, Lin J, van Holsbeeck MT, Hayes CW: US of soft-tissue foreign bodies and associated complications with surgical correlation. *Radiographics* 2001; 21: 1251–1256. doi: 10.1148/radiographics.21.5.g01se271251.
- Kang BS, Shim HS, Kim JH, Kim YM, Bang M, Lim S *et al.*: Angioleiomyoma of the extremities: findings on ultrasonography and magnetic resonance imaging. *J Ultrasound Med* 2019; 38: 1201–1208. doi: 10.1002/jum.14798.
- Omar IM, Weaver JS, Altbach MI, Herynk BA, McCurdy WE, Kadakia AR *et al.*: Imaging of osteoarthritis from the ankle through the midfoot. *Skeletal Radiol* 2023; 52: 2239–2257. doi: 10.1007/s00256-023-04287-7.
- Salet E, Legghe B, Barouk P, Stigliz Y, Dallaudiere B, Lintingre PF *et al.*: Imaging of the post-operative hallux valgus: what do radiologists need to know? *Skeletal Radiol* 2023; 52: 1629–1637. doi: 10.1007/s00256-023-04322-7.
- Bloem JL, Reijnierse M, Huizinga TWJ, van der Helm-van Mil AHM: MR signal intensity: staying on the bright side in MR image interpretation. *RMD Open* 2018; 4: e000728. doi: 10.1136/rmdopen-2018-000728.
- Colebatch AN, Edwards CJ, Ostergaard M, van der Heijde D, Balint PV, D'Agostino MA *et al.*: EULAR recommendations for the use of imaging of the joints in the clinical management of rheumatoid arthritis. *Ann Rheum Dis* 2013; 72: 804–814. doi: 10.1136/annrheumdis-2012-203158.
- Nieuwenhuis WP, van Steenbergen HW, Mangnus L, Newsum EC, Bloem JL, Huizinga TWJ *et al.*: Evaluation of the diagnostic accuracy of hand and foot MRI for early rheumatoid arthritis. *Rheumatology* 2017; 56: 1367–1377. doi: 10.1093/rheumatology/kex167.
- Dakkak YJ, Boeters DM, Boer AC, Reijnierse M, van der Helm-van Mil AHM: What is the additional value of MRI of the foot to the hand in undifferentiated arthritis to predict rheumatoid arthritis development? *Arthritis Res Ther* 2019; 21: 56. doi: 10.1186/s13075-019-1845-7.
- Boeren AMP, Niemantsverdriet E, Verstappen M, Wouters F, Bloem JL, Reijnierse M *et al.*: Towards a simplified fluid-sensitive MRI protocol in small joints of the hand in early arthritis patients: reliability between modified Dixon and regular Gadolinium enhanced TSE fat saturated MRI-sequences. *Skeletal Radiol* 2023; 52: 1193–1201.
- Ohrndorf S, Boer AC, Boeters DM, ten Brinck RM, Burmester G-M, Kortekaas MC *et al.*: Do musculoskeletal ultrasound and magnetic resonance imaging identify synovitis and tenosynovitis at the same joints and tendons? A comparative study in early inflammatory arthritis and clinically suspect arthralgia. *Arthritis Res Ther* 2019; 21: 59. doi: 10.1186/s13075-019-1824-z.
- Dakkak YJ, Niemantsverdriet E, van der Helm-van Mil AHM, Reijnierse M: Increased frequency of intermetatarsal and submetatarsal bursitis in early rheumatoid arthritis: a large case-controlled MRI study. *Arthritis Res Ther* 2020; 22: 277. doi: 10.1186/s13075-020-02359-w.
- Prevoo ML, van 't Hof MA, Kuper HH, van Leeuwen MA, van de Putte LB, van Riel PL: Modified disease activity scores that include twenty-eight-joint

- counts. Development and validation in a prospective longitudinal study of patients with rheumatoid arthritis. *Arthritis Rheum* 1995; 38: 44–48. doi: 10.1002/art.1780380107.
40. Mandl P, Naredo E, Wakefield RJ, Conaghan PG, D'Agostino MA, OMERACT Ultrasound Task Force: A systematic literature review analysis of ultrasound joint count and scoring systems to assess synovitis in rheumatoid arthritis according to the OMERACT filter. *J Rheumatol* 2011; 38: 2055–2062. doi: 10.3899/jrheum.110424.
41. Zufferey P, Brulhart L, Tamborrini G, Finckh A, Scherer A, Moller B *et al.*: Ultrasound evaluation of synovitis in RA: correlation with clinical disease activity and sensitivity to change in an observational cohort study. *Joint Bone Spine* 2014; 81: 222–227. doi: 10.1016/j.jbspin.2013.08.006.